The Geological Society of America
Special Paper 463
2010

Timing and mechanisms of basement uplift and exhumation in the Colorado Plateau–Basin and Range transition zone, Virgin Mountain anticline, Nevada-Arizona

Mark C. Quigley*
Department of Geological Sciences, University of Canterbury, Christchurch 8140, New Zealand

Karl E. Karlstrom*
Department of Earth and Planetary Sciences, University of New Mexico, Albuquerque, New Mexico 87131, USA

Shari Kelley*
Matt Heizler*
New Mexico Institute of Technology, Socorro, New Mexico 87801, USA

ABSTRACT

Structural, stratigraphic, and thermochronologic studies provide insight into the formation of basement-cored uplifts within the Colorado Plateau–Basin and Range transition zone in the Lake Mead region. Basement lithologic contacts, foliations, and ductile shear zones preserved in the core of the Virgin Mountain anticline parallel the trend of the anticline and are commonly reactivated by brittle fault zones, implying that basement anisotropy exerted a strong influence on the uplift geometry of the anticline. Potassium feldspar $^{40}Ar/^{39}Ar$ thermochronology indicates that basement rocks cooled from ≥250–325 °C to ≤150 °C in the Mesoproterozoic and remained at shallow crustal levels (<5–7 km) until they were exhumed to the surface. Apatite fission-track ages and track length measurements reveal a transition from slow cooling beginning at 30–26 Ma to rapid cooling at ca. 17 Ma, which we interpret to mark the change from regional post-Laramide denudational cooling to rapid extension-driven exhumational cooling by ca. 17 Ma. Middle Miocene conglomerates (ca. 16–11 Ma) flanking the anticline contain locally derived basement clasts with ca. 20 Ma apatite fission-track ages, implying rapid exhumation rates of ≥500 m m.y.$^{-1}$. The apparently complex geometry of the anticline resulted from the superposition of first-order processes, including isostatic footwall uplift and extension-perpendicular shortening, on a previously tectonized and strongly anisotropic crust. A low-relief basement-cored uplift may have formed during the Late Cretaceous–early Tertiary Laramide orogeny; however, the bulk of uplift, exhumation, and deformation of the Virgin Mountain anticline occurred during middle Miocene crustal extension.

*E-mails: Quigley: qdownunda@hotmail.com; Karlstrom: kek1@unm.edu; Kelley: zaftkelley@aol.com; Heizler: matt@nmt.edu.

Quigley, M.C., Karlstrom, K.E., Kelley, S., and Heizler, M., 2010, Timing and mechanisms of basement uplift and exhumation in the Colorado Plateau–Basin and Range transition zone, Virgin Mountain anticline, Nevada-Arizona, *in* Umhoefer, P.J., Beard, L.S., and Lamb, M.A., eds., Miocene Tectonics of the Lake Mead Region, Central Basin and Range: Geological Society of America Special Paper 463, p. 311–329, doi: 10.1130/2010.2463(14). For permission to copy, contact editing@geosociety.org.

INTRODUCTION

This paper uses structural, stratigraphic, and thermochronologic data to investigate the uplift and exhumation history of the Virgin Mountain anticline, one of a series of enigmatic basement-cored uplifts outcropping within the Colorado Plateau–Basin and Range transition zone in the Lake Mead region (Fig. 1). Paleoproterozoic plutonic and metamorphic basement rocks within this region are exposed in uplifted culminations with outcrop areas that range from ~5 to 400 km^2 (Fig. 1). These uplifts define dramatic undulations in the vertical structural relief of the Proterozoic basement–Paleozoic cover contact or Great Unconformity (Powell, 1875), a datum that was several kilometers below sea level and subhorizontal prior to Late Cretaceous to early Cenozoic Laramide tectonism. During the Late Cretaceous, this surface was uplifted, tilted toward the northeast, and erosionally beveled such that basement rocks were exposed (by the early Eocene) in the Mogollon highlands to the south (Young, 2001) (Fig. 1). Basement rocks today reach highest elevations in the core of the Virgin Mountain anticline (2.4 km), the Gold Butte block (1.6 km), and in ranges of the Arizona transition zone (Mogollon highlands, 2.5 km; Fig. 1). Across a large region of the western Grand Canyon, the Great Unconformity is at a relatively constant elevation of approximately 0.4 km (Fig. 1). This surface is downdropped to ~3–4 km below sea level in the Grand Wash Trough and may be as deep as ~7 km below sea level in the hanging wall of the Piedmont fault in the eastern Virgin River depression, as inferred from seismic-reflection data (Fig. 1; Bohannon et al., 1993; Langenheim et al., 2001). The vertical undulations and offsets of the Great Unconformity datum thus exceed 5 km, and may reach as much as 9 km, over horizontal distances of <20 km, defining some of the most pronounced structural topography in the continental United States. Despite considerable interest (e.g., Moore, 1972; Wernicke and Axen, 1988; Anderson and Barnhard, 1993;

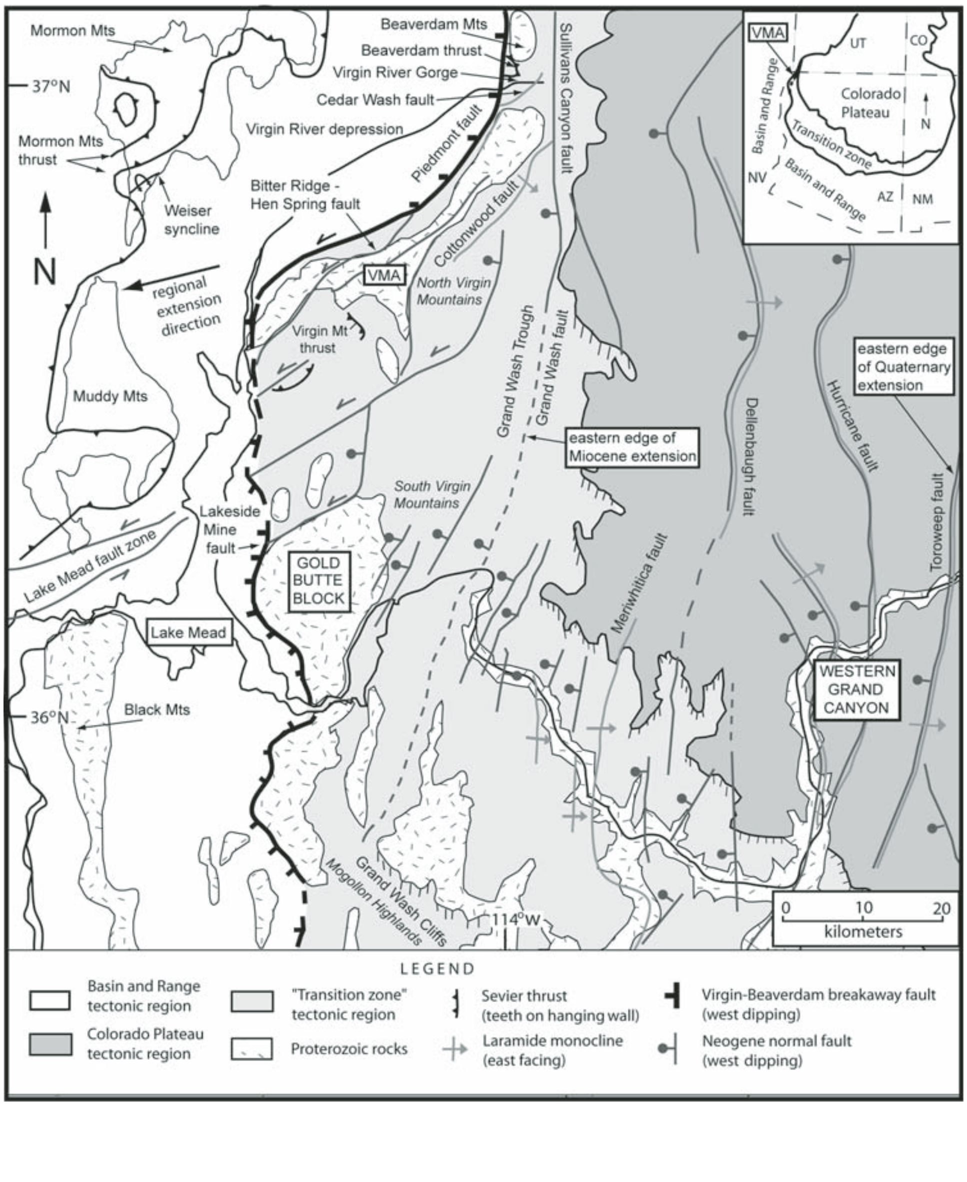

Figure 1. Tectonic map of the Lake Mead area and Colorado Plateau–Basin and Range transition zone, showing locations of basement-cored uplifts and major faults. VMA—Virgin Mountain anticline. See text for details. Geology was modified from Moore (1972), Huntoon (1990), Beard (1996), and Kamilli and Richard (1998).

Anderson et al., 1994; Campagna and Aydin, 1994; Duebendorfer et al., 1998; Brady et al., 2000; Langenheim et al., 2001), the timing and origin of formation of this structural topography are unresolved and highly controversial.

Early workers in the Lake Mead region proposed that basement-cored uplifts such as the Virgin Mountain anticline and Beaver Dam Mountains (Fig. 1) formed in response to approximately E-W contraction during the Late Cretaceous–early Tertiary Laramide orogeny (Beal, 1965; Moore, 1972; Hintze, 1986). Subsequent studies documented the presence of deformed Miocene sedimentary rocks on the flanks of basement uplifts and concluded that the observed uplift was primarily the result of Neogene approximately ENE-WSW extension (Wernicke and Axen, 1988). Structural (Anderson and Barnhard, 1993; Anderson et al., 1994; Campagna and Aydin, 1994; Brady et al., 2000), stratigraphic (Beard, 1996), and thermochronologic studies (Fitzgerald et al., 1991; Reiners et al., 2000) suggested that basement rocks were uplifted and exhumed in the Miocene, but the processes responsible for uplift are debated. Proposed uplift mechanisms include (1) isostatic uplift of tectonically denuded footwalls during crustal extension (Wernicke and Axen, 1988; Brady et al., 2000); (2) complex strain fields involving synchronous ENE-WSW extension and N-S shortening (Wernicke et al., 1985) with structural "crowding" of laterally translated basement blocks (Anderson and Barnhard, 1993); (3) linked strike-slip and normal faulting (Campagna and Aydin, 1994; Beard, 1996; Duebendorfer et al., 1998); and (4) passive upper-crustal responses to middle- or lower-crustal flow (Kruse et al., 1991; Anderson et al., 1994; Langenheim et al., 2001). These proposed models are not mutually exclusive; however, each has different implications for the mechanisms of crustal extension and uplift in one of the world's classic and most cited extensional terranes.

In this paper, we present new structural and stratigraphic mapping and new K-feldspar $^{40}Ar/^{39}Ar$ and apatite fission-track thermochronology from the Virgin Mountain anticline. Our results are compared with previous studies of nearby basement terranes within the Gold Butte block in the South Virgin Mountains (Fryxell et al., 1992; Fitzgerald et al., 1991; Reiners et al., 2000) and western Grand Canyon (Kelley et al., 2001) to better understand how spatial and temporal patterns of tectonism and exhumation varied within the Colorado Plateau–Basin and Range transition zone.

GEOLOGIC SETTING

The Lake Mead region of northeast Nevada and northwest Arizona exposes the structural transition from the weakly extended Colorado Plateau to the highly extended Basin and Range Province (Fig. 1). The Colorado Plateau consists of a basement of Proterozoic schist, gneiss, and granite nonconformably overlain by an ~1–3-km-thick, gently northeast-tilted (<5°) Paleozoic sedimentary sequence and an ~1–2-km-thick Mesozoic sedimentary sequence. Isolated fault-bounded remnants of gently deformed Mesoproterozoic and Neoproterozoic strata are locally present between Proterozoic basement and the Paleozoic section (e.g., Timmons et al., 2001, 2005). The plateau contains widely spaced (10–20 km spacing) basement-penetrating reverse and normal faults that exhibit Proterozoic, Mesozoic, and Cenozoic movement histories, indicating a long history of brittle fault reactivation (e.g., Huntoon, 1990; Marshak et al., 2000; Timmons et al., 2001). The Basin and Range consists of extensional allochthons of thicker Neoproterozoic, Paleozoic, and Mesozoic stratigraphy bound by normal and strike-slip faults (e.g., Wernicke et al., 1988). The Colorado Plateau–Basin and Range transitional boundary in the South Virgin Mountains is sharp and defined by the Grand Wash fault and Grand Wash Cliffs (Longwell et al., 1965). In the North Virgin Mountains, the boundary is more gradational, consisting of a region of small-offset (<1 km) normal faults between the Grand Wash fault and the Piedmont fault–Virgin–Beaver Dam breakaway zone (Fig. 1; Moore, 1972; Wernicke and Axen, 1988). In this paper, we classify the Colorado Plateau–Basin and Range transition zone north of Lake Mead as the region between the Grand Wash fault and the major normal fault systems defining the western edge of the Virgin Mountain anticline (Piedmont fault) and Gold Butte block (Lakeside Mine fault; Fig. 1). Estimates of regional crustal extension based on restored cross sections range from ~73% (approximately 15.8 km) in the South Virgin Mountains (Brady et al., 2000) to ~55% (7.5 km) across the northern part of the Virgin Mountain anticline (as interpreted from the cross sections of Bohannon et al., 1993). The direction of extension in the vicinity of the Virgin Mountain anticline is inferred to be ENE-WSW (Anderson and Barnhard, 1993; Wernicke et al., 1985; Michel-Noel, 1988; Duebendorfer et al., 1998).

A wide array of structures is present within the transition zone. North- to northeast-trending normal and left-lateral faults crosscut Proterozoic to Quaternary lithologies and interact with Neogene synextensional basins, implying ENE-WSW–directed Miocene to Holocene extension (Moore, 1972; Anderson, 1973; Bohannon, 1979; Anderson and Barnhard, 1993; Beard, 1996; Brady et al., 2000). Wernicke and Axen (1988) interpreted some of the steep north- to northeast-trending faults as accommodating displacement driven by isostatic rebound. Arcuate reverse and normal faults with approximately E-W–trending segments and approximately E-W–trending folds displace basement and cover sequences and are interpreted to reflect zones of Miocene contraction and differential uplift at a high angle to the direction of extension (Anderson and Barnhard, 1993). North- to northeast-trending thrust and reverse faults crosscut Proterozoic to Mesozoic lithologies and are interpreted to have formed during Cretaceous to early Tertiary E-W contraction (Beal, 1965; Moore, 1972). Mesozoic thrust faults to the west of the transition zone were variably reactivated as low-angle normal faults during Miocene extension (Wernicke et al., 1984; Axen, 1991; Anderson and Barnhard, 1993).

The Gold Butte block has been the subject of numerous geologic studies and provides a proximal geologic context for the investigation of the lesser studied Virgin Mountain anticline. Basement rocks within the Gold Butte block include 1.7–1.8 Ga gneisses (Wasserburg and Lamphere, 1965; Bennett and DePaolo, 1987) intruded by a large ca. 1.45 Ga granite pluton (Silver et al., 1977). Basement is unconformably overlain to the east by steeply east-dipping Paleozoic to Miocene sedimentary rocks of similar thickness to the Colorado Plateau sequences (Brady et al., 2000). Thermobarometry of gneisses immediately beneath the unconformity indicates pressures of 2–3 kbar, while samples 12–13 km to the west indicate pressures of 5–6 kbar, suggesting that the Gold Butte block is an exhumed Proterozoic-Miocene crustal cross section of up to 15 km paleodepth (Fryxell et al., 1992). Apatite fission-track ages decrease from ca. 50 Ma immediately beneath the unconformity to ca. 17 Ma at a depth of ~1.4 km and remain at ca. 14–17 Ma to a depth of 12.7 km (Fitzgerald et al., 1991). Apatite (U-Th)/He ages are ca. 15 Ma throughout the block (Reiners et al., 2000). On the basis of structural interpretations, Wernicke and Axen (1988) and Brady et al. (2000) hypothesized that the Gold Butte block was isostatically uplifted in response to Miocene tectonic denudation associated with top-to-the-west normal faulting. Recent $^{40}Ar/^{39}Ar$ thermochronologic and structural studies (Karlstrom et al., 2001) and aluminum-in-hornblende barometric studies (Brady, 2005) have argued for shallower basement paleodepths and suggested that the thermobarometric conditions determined by Fryxell et al. (1992) may have been influenced by Proterozoic tectonism (see Karlstrom et al., this volume).

VIRGIN MOUNTAIN ANTICLINE

Geometry and Geology

The Virgin Mountain anticline consists of three elongate basement culminations that constitute an anticlinal “core” variably overlain by outward-dipping autochthonous and allochthonous sections of Paleozoic strata that comprise anticlinal “limbs.” From south to north, the Black Ridge basement culmination trends northeast (oblique to the regional ENE-WSE extension direction), the North Virgin culmination trends east-northeast (roughly parallel to the extension direction), and the Mount Bangs culmination trends north-northeast (highly oblique to the extension direction) (Fig. 2). Basement rocks at culmination crests are situated up to 3.5 km higher than rocks in the intervening structural saddles, such as the Virgin River Gorge (Figs. 1 and 2) (Anderson and Barnhard, 1993), where basement rocks are locally overlain by up to 2 km of Paleozoic strata. Basement rocks immediately east of the anticline reside at depths of almost 6 km below equivalent rocks at culmination crests (Wernicke and Axen, 1988), attesting to the high structural relief across this structure.

Basement rocks within the Virgin Mountain anticline include strongly foliated granite gneiss, amphibolite gneiss, and metasedimentary gneiss, and schist, including pelites, psammites, marbles, and cherts (Beal, 1965; Moore, 1972; Quigley et al., 2002; Quigley, 2002). Preliminary U/Pb monazite geochronology and structural-petrologic studies (Quigley, 2002) indicate that these rocks were deformed and metamorphosed at ca. 1.8–1.6 Ga and correlate with Colorado Plateau basement rocks (Ilg et al., 1996). Lithologic contacts and predominant foliations trend primarily to the northeast in the Black Ridge culmination, east-northeast in the North Virgin culmination, and north to north-northeast in the Mount Bangs culmination, parallel to the trend of the anticline segments (Fig. 2). Foliation-parallel ductile shear zones are present in all domains (Quigley, 2002). On the outcrop scale, lithologic contacts, foliation planes, and shear zones have been variably reactivated by brittle faults (see next section).

The basement core of the Virgin Mountain anticline is overlain by deformed Lower Paleozoic to Upper Cenozoic sedimentary and volcanic rocks that collectively define the anticlinal geometry. The nature of the basement-cover contact varies dramatically throughout the anticline. In places, basal Tapeats Sandstone is in depositional contact with basement (Fig. 2), similar to Grand Canyon. In other places, basement is separated from the Tapeats Sandstone and overlying Bright Angel Shale by bedding-parallel fault zones, implying structural decoupling of basement from cover. The Tapeats and Bright Angel units are commonly crosscut by bedding-parallel and high-angle normal faults, indicating structural thinning of the Lower Paleozoic succession (Fig. 3). However, in most places, basement is in fault contact with strongly deformed Upper Paleozoic or Mesozoic strata, or it is juxtaposed with Tertiary sedimentary rocks (Fig. 2). Various normal, strike-slip, and thrust faults are present along the contacts (Beal, 1965; Moore, 1972; Anderson and Barnhard, 1993). Faults within the cover sequence with map traces at a high angle to basement foliation trajectories do not continue into underlying basement, suggesting that these structures sole into regional detachments in the Lower Cambrian sequence and at the basement-cover contact (Fig. 3). This style of deformation is documented at outcrop scale (Fig. 3) and may also be present in the adjacent Gold Butte block (Brady et al., 2000; Karlstrom et al., 2001).

Faults and Folds

Variably oriented thin-skinned (Sevier-style) thrust faults, basement-penetrating (Laramide-style) reverse faults, normal faults (high angle and listric), and strike-slip faults are all present in the Virgin Mountain anticline region (Fig. 2). Low-angle thrust faults (Beaver Dam thrust and Virgin Mountain thrust; Fig. 1) and fault-related N-S–trending folds imply approximately E-W shortening and likely formed during the Mesozoic Sevier orogeny (Moore, 1972; Axen et al., 1990). East- and northeast-striking reverse faults (Cedar Wash fault, Cottonwood fault; Seager, 1970; Moore, 1972; Beard, 1993) (Fig. 1) and east- to northeast-trending folds (Anderson and Barnhard, 1993) imply NW-SE to N-S shortening. Moore (1972) proposed a Laramide origin for these structures; however, similar structures deform Miocene rocks of the region, suggesting that many of these features formed in response to approximately N-S shortening accom-

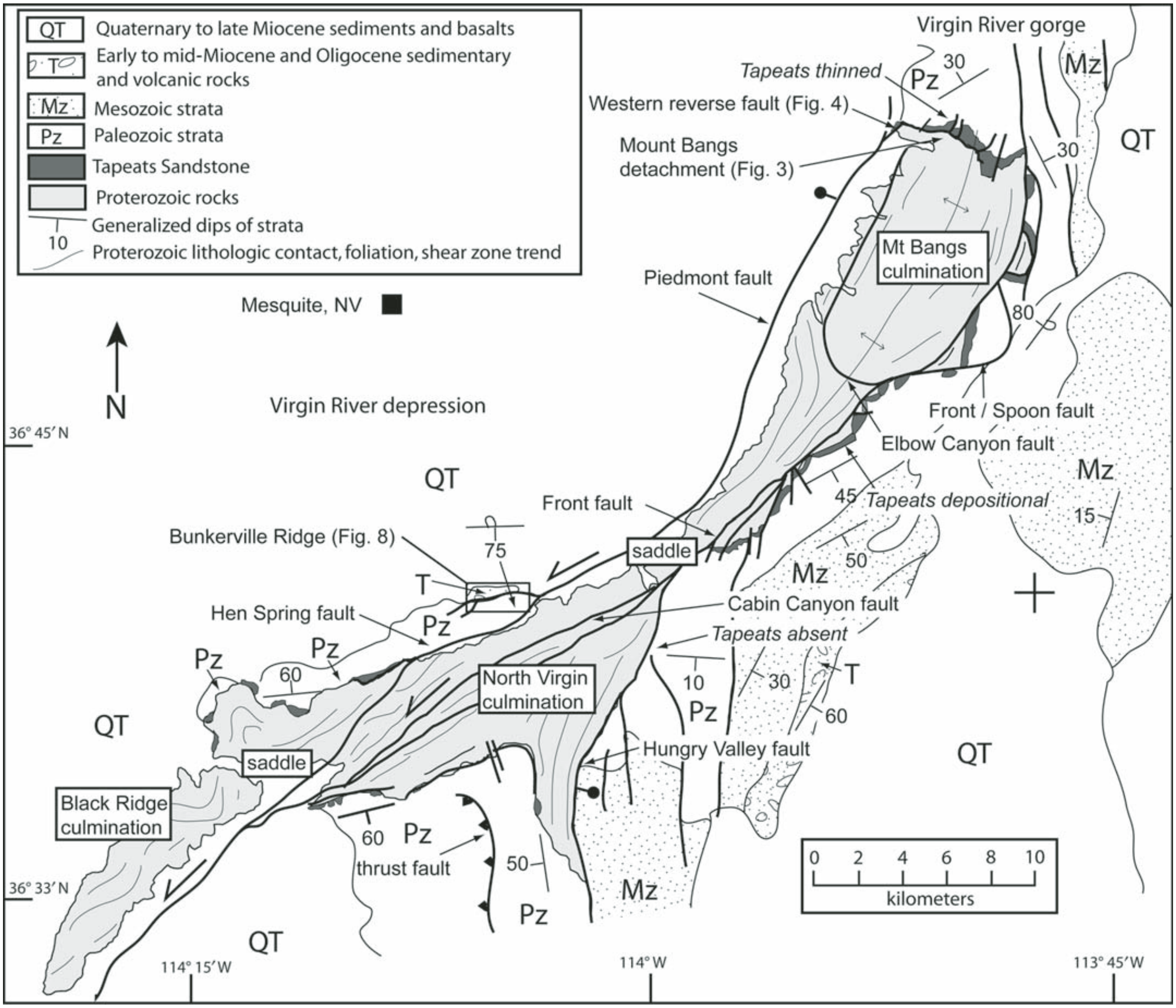

Figure 2. Geology of the Virgin Mountain anticline, including location of major faults described in the text and basement lithologic contacts, foliation, and shear zone trajectories. The anticline is segmented into the Black Ridge, North Virgin, and Mount Bangs culminations, separated by topographically low structural saddles (Anderson and Barnhard, 1993). Selected representative sites where basal Tapeats Sandstone is in depositional contact (Tapeats depositional) and faulted contact (Tapeats thinned) or absent (Tapeats absent) are shown.

panying Miocene extension (Wernicke et al., 1985; Anderson and Barnhard, 1993; Anderson et al., 1994). North-northeast– to east-northeast–striking left-lateral strike-slip faults (e.g., Bitter Ridge–Hen Spring fault, Cabin Canyon fault; Figs. 1 and 2) make up the northern part of the Lake Mead fault system, a major mid-Miocene to Pleistocene left-lateral fault network with a proposed offset of up to ~60 km (Anderson, 1973; Bohannon, 1979). Left-lateral faults are kinematically linked with N-S–striking normal faults (e.g., Piedmont fault) and subordinate northwest-striking right-lateral faults (Duebendorfer and Wallin, 1991; Beard, 1996), collectively defining a Miocene strain field characterized by approximately ENE-WSW extension and approximately N-S shortening (Wernicke et al., 1985, 1988; Anderson and Barnhard, 1993). Beard (1996) concluded that left-lateral and normal faulting initiated at ca. 16–14 Ma based on facies relations in synextensional basin deposits. Anderson and Barnhard (1993) suggested that many of the normal and strike-slip faults in the cover sequence reflect structural collapse into the voids created by lateral basement translations, and that some of the Virgin Mountain anticline basement culminations are dissected by arcuate convex-upward faults (Elbow Canyon fault; Fig. 2) that accommodated relative tilting of adjacent basement blocks.

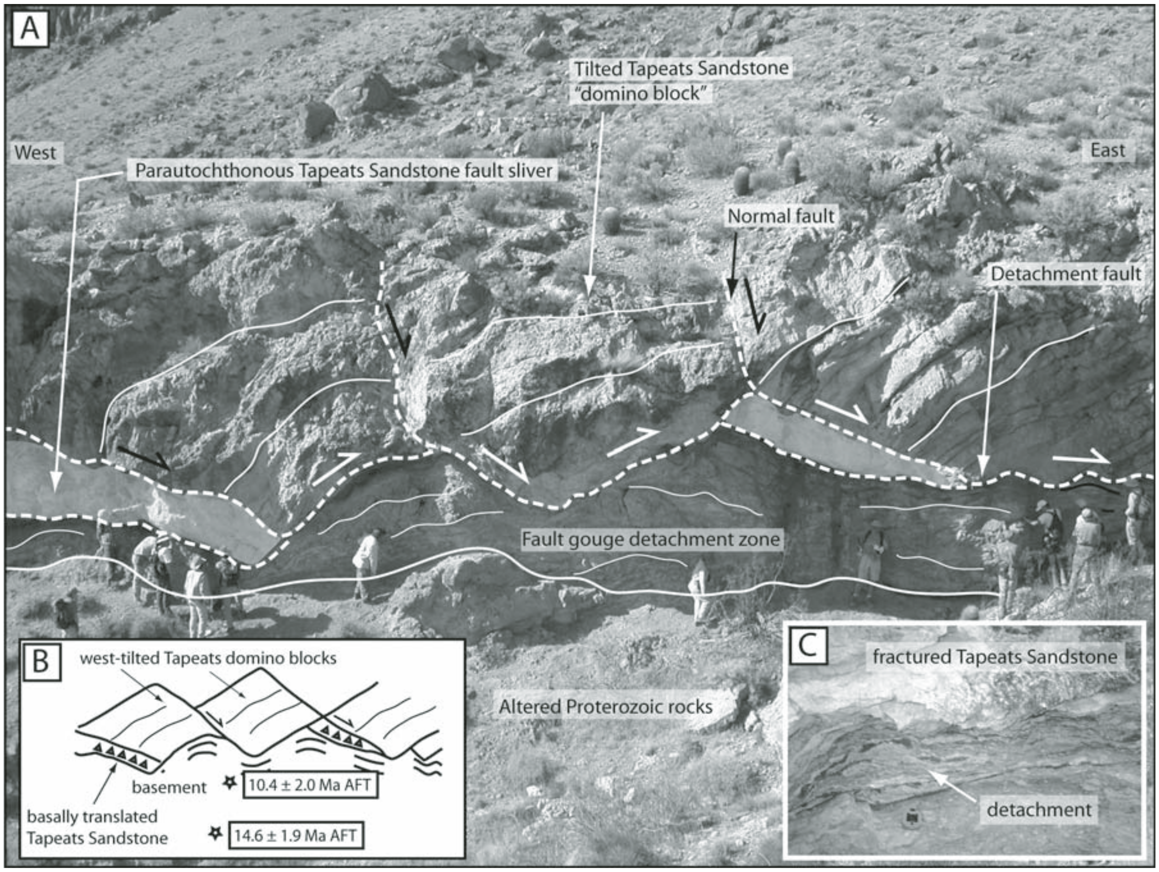

Figure 3. (A) Field photograph of the Mount Bangs detachment, looking north. Normal faults crosscutting west-tilted Tapeats Sandstone "domino" blocks sole into a subhorizontal detachment fault near the Great Unconformity. Subhorizontal Tapeats blocks beneath rotated blocks are interpreted to be semi-autochthonous blocks that were basally translated along the detachment. (B) Schematic interpretative sketch of the outcrop, showing location of apatite fission-track (AFT) samples QFT 24A and QFT 24B. See text for details. (C) Fine-grained detachment fault gouge composed of low-grade alteration minerals (clays); contains numerous conjugate normal faults and shear bands related to semiductile extensional faulting. Kinematic indicators suggest approximately E-W extension.

The Cabin Canyon fault reactivates the Paleoproterozoic Virgin Mountain shear zone along its strike length (Quigley, 2002). To the northeast, the Front fault reactivates a ductile shear zone at the contact between granitic and metasedimentary gneiss. The Hen Spring, Hungry Valley, and Piedmont faults all parallel basement foliation trends and presumably have utilized these anisotropies to facilitate brittle fracturing. From these observations, we suggest that basement anisotropy played a strong role in governing the orientation of some of the major fault structures within the Virgin Mountain anticline. Because some of these faults accommodate major uplift, this suggests that basement anisotropy was important in influencing the uplift geometry of the anticline.

Newly Recognized Faults and Their Kinematic Significance

We identified two previously undocumented faults that have important implications for the tectonic evolution of the Virgin Mountain anticline. At the north end of the anticline, Paleozoic rocks girdle the NNE-plunging nose of the Mount Bangs culmination (Fig. 2). At the basement-cover contact in this area, series of west-tilted allochthonous fault blocks of Tapeats Sandstone are separated by steeply east-dipping normal faults that sole into a flat-lying ~2–3-m-thick fault gouge zone (Fig. 3). Bedding planes of fault-bounded slivers of Tapeats Sandstone immediately above the gouge zone are subparallel to the detachment zone and occur at a high angle to bedding in the overlying sandstone blocks, suggesting that the slivers have been mechanically separated from the overlying blocks and translated eastward along a shallow-dipping detachment zone. Fault block corners plunge gently (5°–15°) toward the north-northeast, suggesting approximately WSW-ENE extension and gentle north-northeast–directed tilting at this locality. Kinematic indicators, including small brittle faults and folds, brittle S-C fabrics, and Reidel shears within the fault gouge zone, are consistent with approximately E-W extension. This fault is referred to as the Mount Bangs detachment, and, along with the bedding-parallel faulting and structural thinning of the basal Cambrian section mentioned already, it is interpreted to indicate that basement culminations were commonly decoupled from the overlying cover sequence during crustal extension. The detachment is part of a large system, where, from east to west, successively younger units are nose-down (west-dipping) against basement. This suggests that the detachment may have moved in a top-to-the-east low-angle domino fashion prior to uplift of the Virgin Mountain anticline. The thickness and intensity of deformation preserved within the fault gouge zone suggest that this is a major fault zone with significant displacement, as opposed to a minor accommodation zone.

The second major fault was discovered at the northwest edge of the Mount Bangs culmination (Western reverse fault; Fig. 2). At this locality, the dip of Lower Paleozoic strata progressively steepens from moderately west dipping (western outcrops), to vertical, to overturned up to 46° toward the southeast (eastern outcrops) against Proterozoic rocks over a distance of ~30 m (Fig. 4). Although no fault plane was directly observed, outcrop relationships necessitate the presence of a southeast-dipping fault with southeast-side-up displacement in order to create the observed geometry and place Proterozoic rocks at equivalent structural levels to adjacent Paleozoic strata (Fig. 4). The geometry of the dipping stratigraphy and inferred orientation of the fault are similar to Laramide monoclines and suggest approximately NW-SE contraction and uplift of basement in the fault hanging wall, assuming contraction was orthogonal to the inferred fault strike and that no significant rotation of the faults occurred during subsequent deformation. The presence of a basement-penetrating reverse fault along the western margin of the anticline implies that a component of basement uplift can be attributed to contractional deformation. The gross geometry and structural trend of the Western reverse fault are similar to many known Laramide faults in the Grand Canyon (Huntoon, 1990), but they are also consistent with the northeast-striking Miocene contractional structures observed elsewhere in the region (Wernicke et al., 1985; Anderson and Barnhard, 1993). We conducted K-feldspar $^{40}Ar/^{39}Ar$ and apatite fission-track thermochronology on uplifted basement rocks to evaluate whether exhumation of the Virgin Mountain anticline occurred during Laramide or Miocene tectonism.

$^{40}Ar/^{39}Ar$ THERMOCHRONOLOGY

Background and Method

The $^{40}Ar/^{39}Ar$ K-feldspar thermochronology method was used to characterize the low-temperature (150–325 °C; Lovera et al., 1989; McDougall and Harrison, 1999) cooling history of Virgin Mountain basement. No prior argon thermochronologic studies had been conducted in this area; however, thermochronology from the nearby Grand Canyon and Gold Butte block basement terranes provides a regional context for this study. Basement thermal histories derived from modeling of $^{40}Ar/^{39}Ar$ K-feldspar age spectra in the eastern Grand Canyon are interpreted to record cooling from ~250–300 °C to below 150 °C between 1300 and 1225 Ma (Timmons et al., 2005). No K-feldspar $^{40}Ar/^{39}Ar$ ages have been published from the Gold Butte block. However, titanite (U-Th)/He thermochronologic ages provide constraints on cooling through similar crustal temperatures (closure temperature ~200 °C; Reiners and Farley, 1999; Reiners et al., 2000) and range from ca. 150–190 Ma at ~3–6 km paleodepths beneath the basement-cover contact to ca. 15–22 Ma at an inferred 14 km paleodepth. Muscovite $^{40}Ar/^{39}Ar$ thermochronologic ages (closure temperature 320–420 °C; Lister and Baldwin, 1996) range from ca. 1368 Ma beneath the unconformity to ca. 91 Ma at inferred 16–18 km paleodepths (Reiners et al., 2000). Collectively, these results indicate that (1) cooling histories for basement rocks immediately below the unconformity in the Gold Butte block and Grand Canyon are similar, and (2) basement rocks from the western Gold Butte block

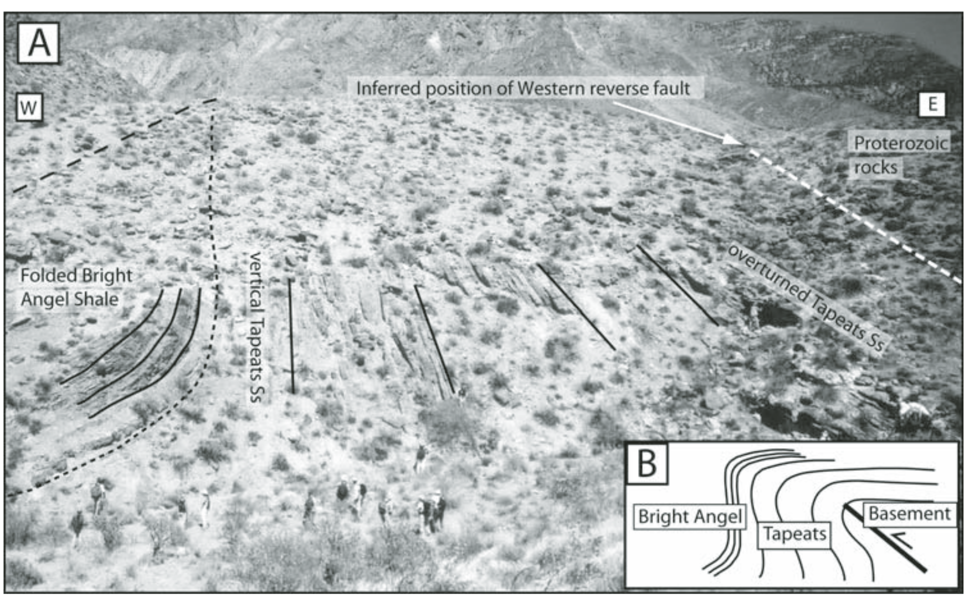

Figure 4. (A) Cross-sectional view of the Western reverse fault at the west limb of the Virgin Mountain anticline, looking north. From west to east, lithologies consist of gently west-dipping Bright Angel Shale, moderately west-dipping to subvertical Bright Angel Shale, subvertical to 46°E-dipping, overturned Tapeats Sandstone in the footwall of the West Monocline reverse fault, and Proterozoic gneiss in the hanging wall of the Western reverse fault. The Western reverse fault is interpreted to dip 46°E, parallel to the dip of drag-folded Tapeats Sandstone at the Cambrian-Precambrian contact. (B) Interpretative schematic of the outcrop.

record Mesozoic and Miocene cooling associated with exhumation of deeper crustal levels (Reiners et al., 2000).

Nine K-feldspar samples from the Virgin Mountain anticline basement were analyzed in this study (Fig. 5). Samples were obtained from immediately beneath autochthonous (QFT 10) and allochthonous (QFT 24b) Tapeats Sandstone, at various elevations perpendicular to the strike of the anticline (QFT 14, 18, 20, 21) and at other locations throughout the anticline (Fig. 5). Samples were step heated at 50 °C increments from 450 to 1685 °C, and argon isotopic analyses were measured on a mass spectrometer using a Daly detector. Our aim was to determine whether feldspar cooling was spatially uniform or variable, and whether cooling occurred in the Mesoproterozoic, similar to the Grand Canyon and the eastern Gold Butte block, or Cretaceous to Miocene, similar to the western Gold Butte block.

Results and Interpretations

K-feldspar age spectra reveal steep age gradients over the initial 10%–20% of ^{39}Ar released, followed by a series of relatively uniform age steps comprising the remaining >80% of the age spectra (Fig. 5). All spectra are dominated by >1000 Ma age steps,

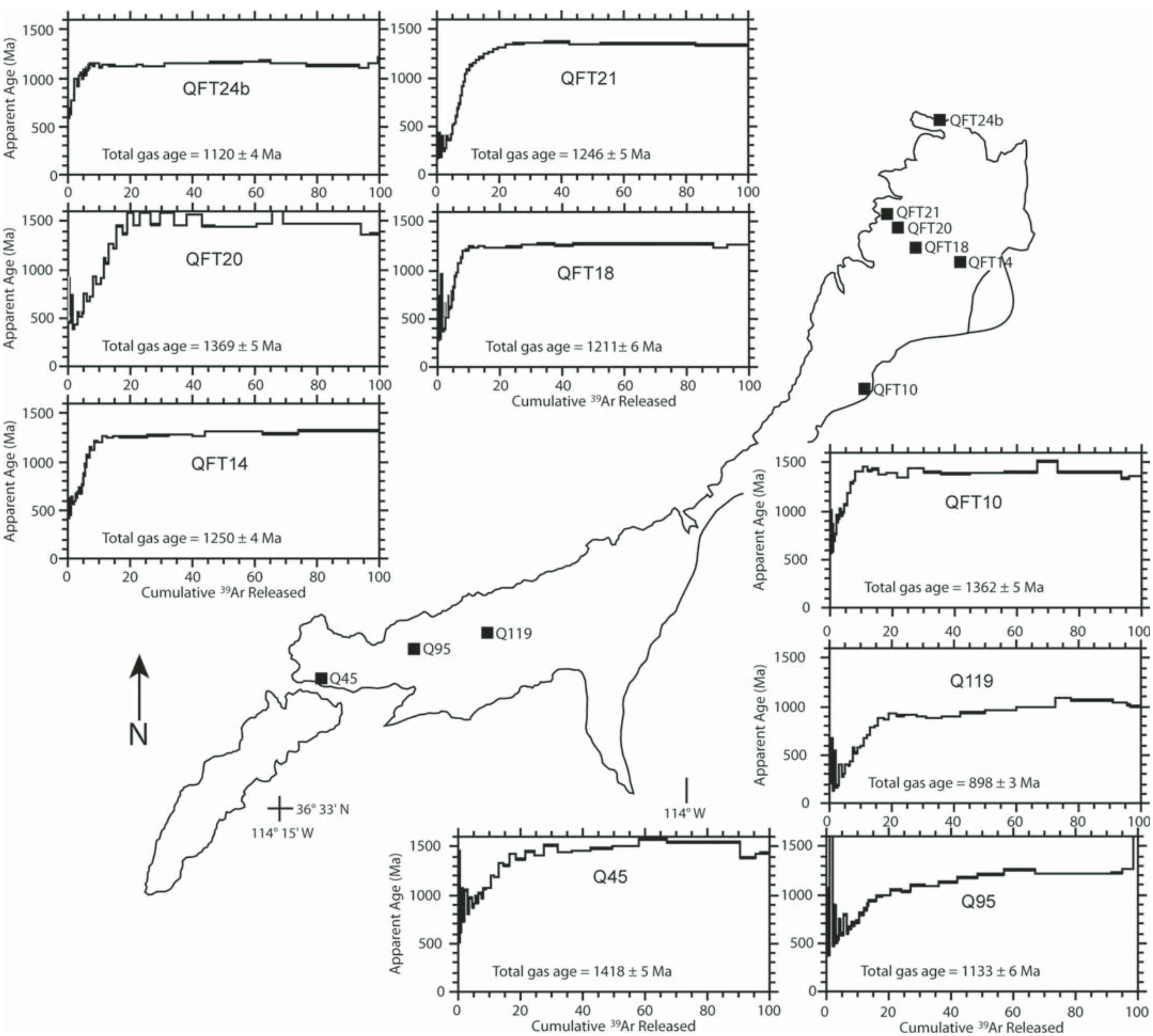

Figure 5. K-feldspar $^{40}Ar/^{39}Ar$ step-heating spectra and sample locations. Minimum ages were derived for lowest $^{40}Ar/^{39}Ar$ ages at or above the 550 °C temperature step.

and the majority of spectra yield step ages of ca. 1300–1500 Ma, suggesting that the basement of the Virgin Mountain anticline cooled from 250 to 325 °C to ~150 °C in the Mesoproterozoic (e.g., Timmons et al., 2005). The younger (<1000–500 Ma) age steps associated with the low-temperature parts of all spectra indicate either that rocks remained at temperatures at or slightly above ~150 °C prior to ca. 500 Ma, *or* that rocks were reheated slightly above ~150 °C at some stage following initial Mesoproterozoic cooling. However, since the young age steps including minimum ages (Fig. 5) account for only a small fraction of the total gas release, any thermal resetting of feldspars was minimal compared to the signal derived from Mesoproterozoic cooling.

Variations in cooling ages between samples (i.e., Q119, which has a total gas age of 898 Ma, versus QFT 24b, which has a total gas age of 1120 Ma) could reflect juxtaposition of slightly different crustal levels following cooling, variations in feldspar chemistry of alteration, and/or fluid-driven temperature variations during or after cooling (Timmons et al., 2005). Intriguingly, samples obtained adjacent to autochthonous Paleozoic cover (QFT 10, Q45) yield older total gas ages than samples obtained from the core of the anticline (e.g., Q119, QFT 18) or samples from beneath allochthonous cover (QFT24b) (Figs. 2 and 5), suggesting that deeper crustal levels might be exposed in the core of the anticline. The data suggest that the Virgin Mountain anticline is not an intact "tilted crustal section" as inferred for Gold Butte, but rather that all rocks exhumed within the anticline were at depths shallower than ~7 km long before Laramide or Miocene tectonism (assuming a geothermal gradient of 20 °C km^{-1} and ambient surface temperature of 10 °C; Fitzgerald et al., 1991; Reiners et al., 2000). Basement rocks within the Virgin Mountain anticline were exhumed from shallower crustal levels than basement rocks exposed in the transition zone in west-central Arizona, which yield Miocene $^{40}Ar/^{39}Ar$ K-feldspar ages (e.g., Foster et al., 1990; Bryant et al., 1991). An important implication of this study is that ductile shear zones within the Virgin Mountain anticline are of Proterozoic age and thus should not be used to investigate the kinematics of Miocene tectonism.

APATITE FISSION-TRACK THERMOCHRONOMETRY

Background and Method

Apatite fission-track (AFT) thermochronometry was used to characterize the cooling history of basement rocks through temperatures of ~60–120 °C (e.g., Naeser, 1979; Green et al., 1989). The AFT age is commonly interpreted as the time at which the sample cooled below the closure temperature and is determined by measuring the density of fission- tracks and the U concentration of the sample. Fission-track lengths reflect the degree of track annealing and are primarily a function of cooling rate; typical track lengths for rapidly cooled samples (>5 °C m.y.$^{-1}$) are >14 μm, while more slowly cooled samples generally yield track lengths <14 μm (e.g., Foster and Gleadow, 1992).

This paper represents the first reported AFT data from the Virgin Mountain anticline. AFT studies of the Gold Butte block (Fitzgerald et al., 1991), western Grand Canyon (Naeser et al., 1989; Kelley et al., 2000, 2001), Beaver Dam Mountains (O'Sullivan et al., 1994; Stockli, 1999), and transition zone in west-central Arizona (Foster et al., 1993) provide a regional context. Samples collected from 0 to 1.2 km beneath the Great Unconformity in the Grand Canyon and Gold Butte block yield 92–34 Ma AFT ages and 13.4–12.8 μm track lengths, indicating slow regional Cretaceous to Oligocene cooling due to progressive erosional unroofing (Fitzgerald et al., 1991; Naeser et al., 1989; Kelley et al., 2000, 2001). Conversely, samples collected below inferred 1.2 km paleodepths beneath the basement unconformity in the Gold Butte block yield 14–17 Ma AFT ages and 14.1–14.7 μm track lengths, indicating rapid Miocene cooling of structurally deeper basement in response to tectonic denudation (Fitzgerald et al., 1991). Apatite fission-track data show that exhumation of the Beaver Dam Mountains basement began at ca. 16 Ma (O'Sullivan et al., 1994; Stockli, 1999). AFT results from the west-central Arizona transition zone include a 107–25 Ma age population with short (<13.5 μm) track lengths and a 21–13 Ma age population with long (>14 μm) track lengths (Foster et al., 1993). These results indicate regional Cretaceous to early Miocene cooling (with possible episodes of reheating) followed by a major, rapid cooling event associated with the onset of extensional faulting at ca. 20 Ma (Foster et al., 1993). Extension onset ages based on thermochronology from the Colorado River extensional corridor in southeastern California and western Arizona range from 23 to 22 Ma (Foster and John, 1999; Foster et al., 1990; Carter et al., 2004, 2006), with an apparent increase in slip rates of extensional faults at ca. 15 Ma (e.g., Carter et al., 2006).

Twenty samples were collected in basement rocks of the Virgin Mountain anticline, including samples immediately beneath the basement unconformity, on opposite sides of major brittle faults, and at various elevations and locations. Two additional samples were collected from bedrock clasts in deformed Miocene sedimentary rocks adjacent to the anticline (see next section). The goal was to determine the spatial and temporal patterns of basement cooling through AFT closure temperatures and to obtain the cooling age of the basement source terrane for the Miocene conglomerates. Apatites were separated and analyzed at the New Mexico Institute of Technology using methods described in Kelley et al. (1992) and Kelley and Chapin (2004). Individual grain ages were calculated using the methods of Hurford and Green (1983). The χ^2 statistic (Galbraith, 1981) was applied to determine whether individual ages belong to a single population. Confined track lengths were measured for 11 of 19 samples (Table 1). Time-temperature histories based on AFT age and track length distributions were modeled for four samples using the AFTsolve computer program of Ketcham et al. (2000) (Fig. 6). Models attempt to reconstruct the cooling path of samples through the partial annealing zone, i.e., temperatures between 60 and 70 °C and 110–140 °C depending on apatite composition and cooling rate.

TABLE 1. APATITE FISSION-TRACK DATA FOR VIRGIN MOUNTAIN ANTICLINE, NEVADA AND ARIZONA

Sample number	Rock type	UTM coordinates	Elevation (m)	Number of grains dated	r_s ($\times 10^5$ t/cm^2)	r_i ($\times 10^6$ t/cm^2)	r_d ($\times 10^5$ t/cm^2)	Central age (Ma, ±1 S.E.)	P(c)^2 (%)	Uranium content (ppm)	Mean track length (mm, ±1 S.E.)	Standard deviation track length (mm)
QFT1	Granodioite gneiss	11 0741414 E 4045720 N	540	20	2.23 (286)	8.32 (5323)	1.148 (4590)	**14.7 ± 1.1**	99	87	13.9 ± 0.4 (61)	1.7
QFT2	Granitic gneiss	11 0743400 E 4048286 N	638	20	0.92 (118)	3.18 (2035)	1.151 (4590)	**15.9 ± 1.6**	99	33	13.7 ± 1.3 (10)	2.1
QFT3B	Quartz diorite	11 0749392 E 4054220 N	855	20	2.06 (264)	7.7 (4929)	1.159 (4590)	**14.8 ± 1.1**	99	80	13.6 ± 0.4 (125)	2.1
QFT4	Mylonitic granite	11 0748044 E 4056172 N	848	5	0.68 (12)	2.29 (202)	1.159 (4590)	**16.4 ± 4.9**	>99	24	–	–
QFT5	Granite below Tapeats ss.	11 0747195 E 4056460 N	755	20	0.9 (115)	2.29 (1466)	1.161 (4590)	**21.7 ± 2.3**	95	24	12.8 ± 0.6 (71)	2.6
QFT6	Mylonite	11 0761956 E 4061148 N	1380	20	0.64 (68)	2.09 (1102)	1.170 (4590)	**17.2 ± 2.3**	98	21	–	–
QFT7	Granodiorite	11 0767184 E 4062385 N	1120	20	0.22 (23)	0.64 (339)	1.170 (4590)	**18.9 ± 4.1**	95	7	12.7 ± 2.0 (14)	3.9
QFT8	Granodiorite	11 0766531 E 4059572 N	1370	20	0.85 (110)	3.21 (2054)	1.175 (4590)	**15.0 ± 1.6**	>99	33	14.7 ± 0.6 (36)	1.9
QFT10	Monzonite and granite	12 0234848 E 4066588 N	1097	20	0.63 (79)	1.76 (1101)	1.176 (4590)	**20.1 ± 2.5**	91	18	13.1 ± 0.7 (61)	2.7
QFT12	Mylonite	12 0239721 E 4074546 N	1173	20	0.36 (46)	1.06 (676)	1.184 (4590)	**19.2 ± 3.1**	99	11	13.4 ± 0.8 (13)	1.4
QFT13	Granitic gneiss	12 0239193 E 4074497 N	1067	13	0.68 (57)	2.71 (1127)	1.186 (4590)	**14.3 ± 2.0**	85	27	–	–
QFT14	Leucogranite Summit Mt. Bangs	12 0245335 E 4075485 N	2443	15	0.46 (34)	1.87 (688)	1.189 (4590)	**14.0 ± 2.5**	99	19	–	–
QFT17	Psammite	12 0244732 E 4075895 N	2138	20	0.77 (99)	2.94 (1883)	1.205 (4590)	**15.1 ± 1.7**	82	29	14.0 ± 0.5 (56)	1.9
QFT19	Psammite	12 0243912 E 4075937 N	1730	20	0.37 (37)	1.43 (708)	1.212 (4590)	**15.1 ± 2.6**	>99	14	13.7 ± 0.8 (19)	1.8
QFT20	Granite	12 0242728 E 4077259 N	1364	20	0.82 (100)	2.80 (1700)	1.220 (4590)	**17.1 ± 1.9**	99	28	14.0 ± 0.6 (16)	1.1
QFT22	Mylonite	12 0241076 E 4078220N	991	20	0.50 (63)	1.75 (1104)	1.221 (4590)	**16.6 ± 2.3**	>99	17	13.8 ± 0.7 (33)	2
QFT23	Biotite schist	12 0243296 E 4083542 N	912	20	0.49 (61)	1.81 (1131)	1.167 (4602)	**15.0 ± 2.1**	>99	19	14.3 ± 1.5 (4)	1.5
QFT24A	Fractured granite	12 0244469 E 4083477 N	1122	11	0.43 (29)	2.31 (776)	1.167 (4602)	**10.4 ± 2.0**	92	24	–	–
QFT24B	Biotite gneiss	12 0244469 E 4083477 N	1119	20	0.66 (68)	2.53 (1296)	1.167 (4602)	**14.6 ± 1.9**	90	26	–	–
QFT 25	Schist Cabin Canyon	11 0762471 E 4059885 N	1525	20	0.18 (16)	0.62 (280)	1.528 (4607)	**20.8 ± 5.4**	95	5	–	–
QFT307a	Granitioid clast Red sandstone	11 0760173 E 4063309 N	1030	20	0.59 (75)	1.89 (1208)	1.542 (4607)	**22.8 ± 2.9**	>99	15	13.8 ± 0.8 (36)	2.5
QFT307b	Granitioid clast Red sandstone	11 0760173 E 4063309 N	1030	8	0.41 (17)	1.51 (314)	1.558 (4607)	**20.1 ± 5.0**	98	12	–	–

Note: r_s—spontaneous track density; r_i—induced track density (reported induced track density is twice the measured density); number in parentheses—number of tracks counted for ages and fluence calibration or the number of track measured for lengths; r_d—track density in muscovite detector covering CN-6 (1.05 ppm), reported value was determined from interpolation of values for detectors covering standards at the top and bottom of the reactor packages (fluence gradient correction); ss—sandstone; S.E.—standard error; P(c)^2—chi-squared probability; – = no data; $l_f = 1.551 \times 10^{-10}$ yr^{-1}, $g = 0.5$; zeta = 4772 ± 340 for apatite. Mean track lengths were not corrected for length bias (Laslett et al., 1982). Unless otherwise noted, the rock units are Proterozoic in age.

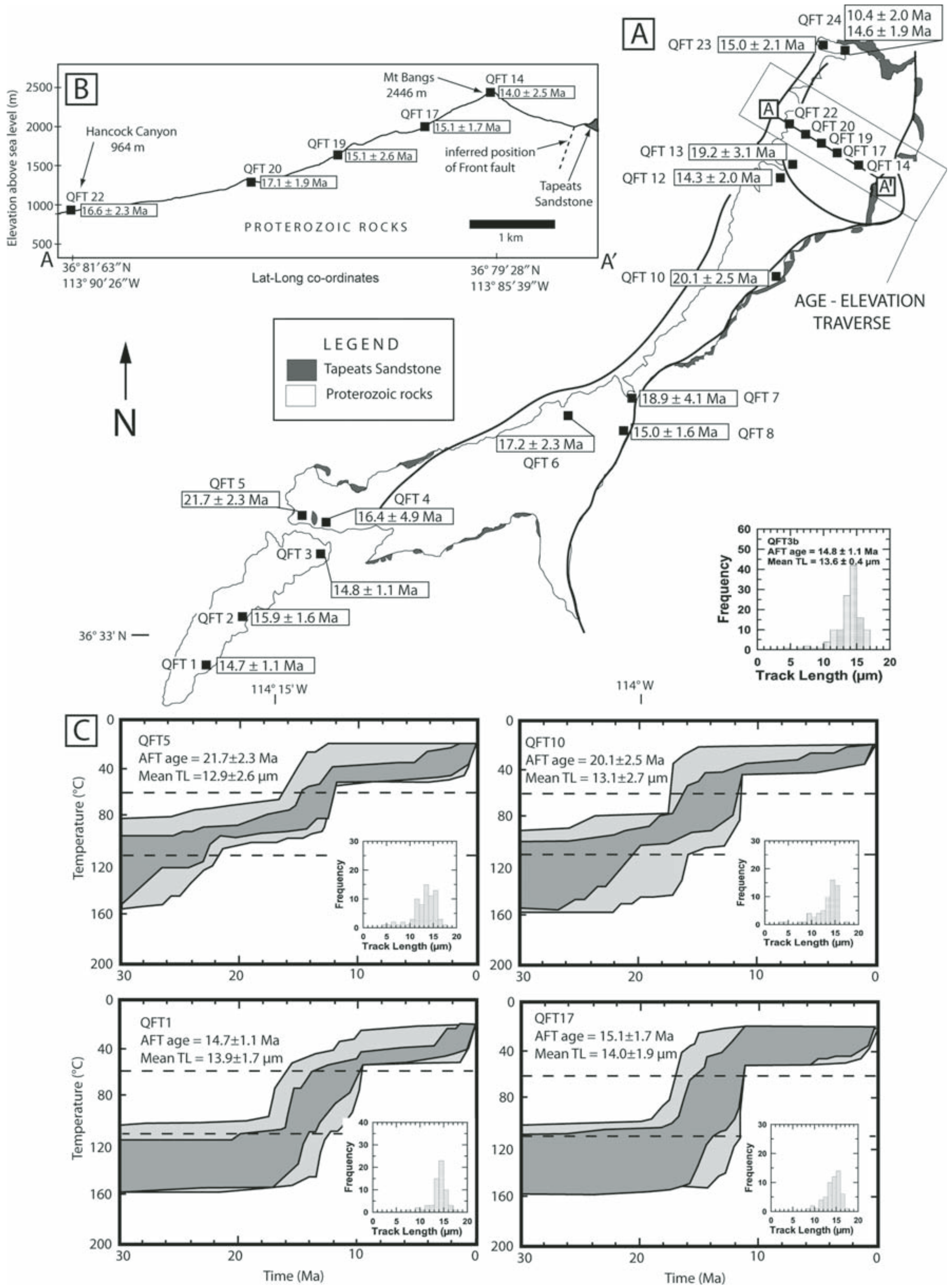

Figure 6. (A) Locations and results of apatite fission-track (AFT) thermochronology from the Virgin Mountain anticline. (B) Locations and results of age-elevation traverse. (C) Modeled temperature histories and track length (TL) distribution plots for basement immediately below the Great Unconformity (QFT5 and QFT10) and basement from a deeper structural level (QFT1 and QFT17). See text for details. No geologic constraints were imposed on the models. The dark-gray areas demarcate a Kolmogorov-Southmirnov (K-south) test probability of 50%, and the light-gray areas demark a K-south probability of 5% (Press et al., 1988; Willett, 1992, 1997; Ketcham et al., 2000). The dashed lines in C delimit the apatite fission-track partial annealing zone.

Results

All AFT ages from the Virgin Mountain basement fall in the range from 21.7 ± 2.3 Ma to 10.4 ± 2.0 Ma, and mean track lengths range from 12.7 ± 2.0 µm to 14.7 ± 0.6 µm (Table 1). Basement clasts yield 22.8 ± 2.9 Ma (mean track length = 13.8 ± 0.8 µm) and 20.1 ± 5.0 Ma ages (Table 1). Basement AFT age–track length relationships define two data groups: older samples (>19 Ma) with shorter track lengths (≤13.4 µm) and younger samples (ca. 14–17 Ma) with longer track lengths (~13.6–14.7 µm) (Figs. 6 and 7). The two oldest samples were collected 1 m (QFT 5) and ~400 m (QFT 10) below the Great Unconformity, where Tapeats Sandstone rests in depositional contact on basement. The next oldest samples were collected at relatively low elevations in the saddle between the Mount Bangs and North Virgin culminations (QFT 7) and on the north side of the proposed Elbow Canyon fault (QFT 12) (Anderson and Barnhard, 1993). Younger samples were obtained from various elevations throughout the Virgin Mountain anticline, including the peak of Mount Bangs (QFT 14), which yielded the second youngest AFT age (Table 1). AFT ages obtained along the NW-SE age-elevation traverse from Mount Bangs to the Piedmont fault are all within analytical error, although the highest elevation samples appear to be the youngest along the profile (Fig. 6B). Samples collected adjacent to the Western reverse fault (QFT 23), Hungry Valley fault (QFT 8), and Mount Bangs detachment (QFT 24A, 24B) yielded young (≤15 Ma) ages. QFT 24A was collected from altered fault gouge within the Mount Bangs detachment (Fig. 3), and we suspect that the anomalously young AFT age of this sample (10.4 ± 2.0 Ma) resulted from alteration and annealing of tracks by fluids within the fault zone, given that the unaltered bedrock sample (QFT 24B) ~5 m below QFT 24A yielded an age ~4 m.y. older (Table 1; Fig. 3). Samples from the North Virgin and Black Ridge culminations range from 17.2 ± 2.3 Ma to 14.7 ± 1.1 Ma and show no systematic relationship with elevation or geographic position (Figs. 6 and 7).

Temperature-time paths (Fig. 6C) were modeled for the two oldest samples (QFT 5, 10) and two of the youngest samples (QFT 1, 17). Models of the oldest samples suggest that rocks immediately beneath the unconformity entered the partial annealing zone (≤110 °C) as early as 30–26 Ma and cooled below 60 °C by ca. 14 Ma. Time-integrated cooling rates for these samples are therefore 3–4 °C m.y.$^{-1}$, although this cooling history is likely to encompass a period of slower cooling (>17 Ma) and more rapid cooling (<17 Ma). Models of the younger samples suggest that rocks remained at temperatures above 110 °C until ca. 17–14 Ma and cooled rapidly from 110 °C to 60 °C by ca. 12 Ma. Cooling rates for these samples are significantly higher (12–25 °C m.y.$^{-1}$) than the older samples. Assuming a geothermal gradient of 20 °C km^{-1} and ambient surface temperature of 10 °C (Fitzgerald et al., 1991; Reiners et al., 2000), the AFT data suggest that basement rocks immediately beneath the Great Unconformity were exhumed from paleodepths of ~5 km to ~2.5 km at rates of ~160–210 m m.y.$^{-1}$, while deeper basement rocks were exhumed through paleodepths of ~5 km to ~2.5 km at rates of ~630–1250 m m.y.$^{-1}$, implying a marked increase in exhumation rate during the middle Miocene. Present exposure of these rocks at the surface implies continued post–12–14 Ma linear exhumation rates of ~180–210 m m.y.$^{-1}$; however, this is not well constrained by the models.

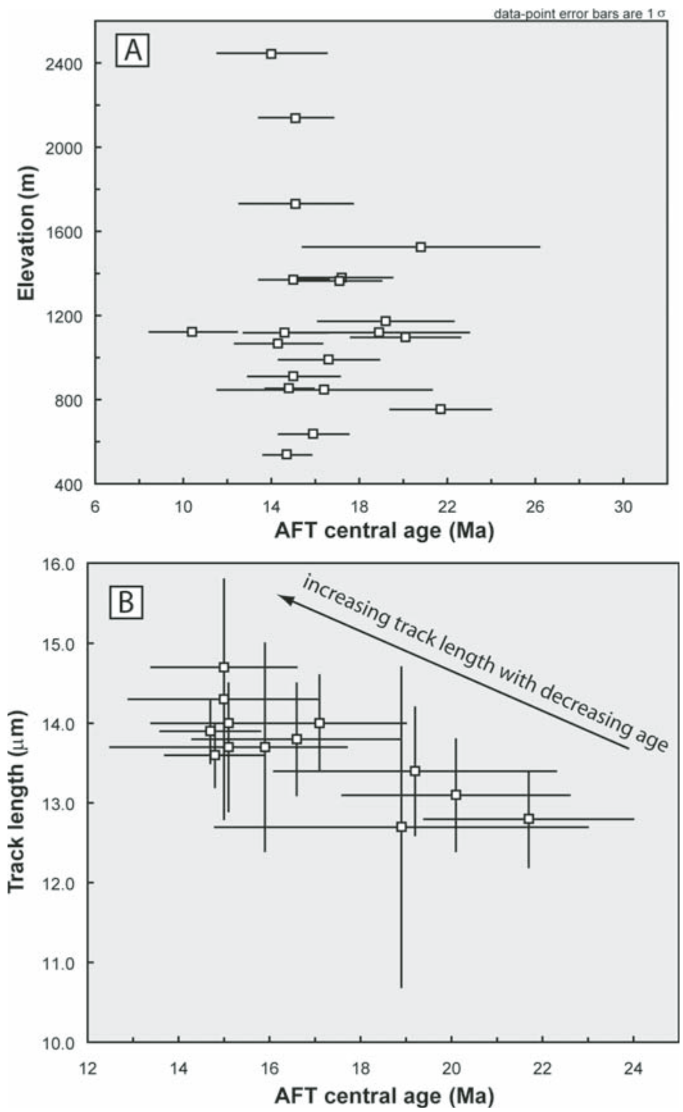

Figure 7. (A) Apatite fission-track (AFT) age versus elevation for bedrock AFT samples from the Virgin Mountain anticline. No clear relationship between age and elevation is present, suggesting that the anticline was actively deforming and uplifting during AFT cooling, as opposed to having cooled entirely following formation. (B) AFT age versus track length plot, showing a general trend toward increased track lengths with decreasing age. This is consistent with increased cooling rates in the middle Miocene (ca. 16–10 Ma; see Fig. 6C) following initial slower cooling of the subunconformity samples at ca. 20 Ma. Only samples with measured track lengths are included. Detrital samples (QFT307a, b) are not included in either plot.

Interpretations

AFT ages, track lengths, and temperature-time models indicate that basement rocks immediately beneath autochthonous Paleozoic cover cooled through the AFT partial annealing zone ~10–16 m.y. earlier at rates as much as ~8–21 °C m.y.$^{-1}$ slower than rocks in structurally deeper parts of the Virgin Mountain anticline, including rocks immediately beneath allochthonous Paleozoic cover (Fig. 6C). This suggests a systematic relationship between basement cooling history and pre-exhumation structural depth, i.e., the structurally shallowest basement rocks cooled slowly in the late Oligocene to early Miocene, while structurally deeper rocks remained at temperatures above the AFT partial annealing zone. The transition from slow to rapid cooling is inferred to have occurred after ca. 22–19 Ma (the age range of short track length samples) and prior to or at ca. 17 Ma (the oldest age of a long track length sample; Table 1). We attribute this increase in cooling rate to the onset of rapid extensional tectonism and rapid basement exhumation at ca. 17 Ma. Prior to ca. 17 Ma, basement exhumation and cooling likely occurred in response to slow erosional denudation and top-down conduction, as indicated by thermal models of the subunconformity, more slowly cooled samples.

Although AFT ages appear to cluster into two groups correlating with structural position, no clear relationship exists between AFT age and sample elevation (Table 1; Fig. 7A). Instead, some of the youngest and most rapidly cooled samples were obtained from the highest elevations in the core of the Virgin Mountain anticline. This suggests that the presently undulating topography of the basement-cover interface developed during or after AFT cooling as the basement rocks in the core of the anticline were uplifted rapidly through AFT closure temperatures beginning around ca. 17 Ma. No evidence for Late Cretaceous–early Tertiary cooling is apparent from basement AFT samples, indicating that any Laramide uplift along basement-bounding reverse faults (Cedar Wash fault, Cottonwood fault, Western reverse fault) did not result in exhumation of basement through temperatures <110 °C.

The relationship of AFT ages to brittle faults provides insight into the crustal level of basement exposed as a result of tectonic denudation. Sample QFT10 (AFT age ca. 20 Ma) was obtained from ~400 m below the Great Unconformity in an area where Tapeats Formation rests depositionally on basement. Assuming this sample provides a reasonable proxy for the time at which rocks at ~400 m paleodepth beneath the Great Unconformity cooled in the Virgin Mountain anticline, samples immediately beneath allochthonous cover that yield younger AFT ages must have had some basement material removed between the sample site and the Great Unconformity. For instance, ≥400 m of basement material must have been tectonically removed within the Mount Bangs detachment in order to juxtapose ca. 15 Ma AFT–age basement with allochthonous cover. This hypothesis can be expanded to suggest that all bedrock sites with ca. 14–16 Ma AFT ages were exhumed from basement situated ≥400 m beneath the Great Unconformity prior to exhumation. An alternative is that subunconformity basement temperatures may have varied spatially, possibly due to varying thicknesses of overlying Paleozoic and Mesozoic strata, although this is harder to reconcile with the limited spatial scale and the nearly overlapping AFT ages.

When considered regionally, AFT ages from immediately beneath autochthonous cover in the Virgin Mountain anticline are considerably younger than structurally equivalent samples in the Grand Canyon (ca. 70–90 Ma) and Gold Butte block (ca. 55 Ma). This indicates that the basement-cover interface in the Virgin Mountain anticline remained at temperatures ≥110 °C tens of millions of years after the equivalent surface cooled below 110 °C elsewhere in the region. In order to explain this relationship, we suggest that Virgin Mountain anticline basement lay beneath a thicker, less denuded sedimentary sequence than adjacent regions prior to Miocene exhumation. This hypothesis is consistent with a pre-Miocene northward dip of the basement-cover contact, as indicated by southward regional beveling of autochthonous Paleozoic and Mesozoic strata at the sub-Tertiary unconformity (Bohannon, 1984) and aerial exposure of Proterozoic basement in the Kingman Uplift south of the Virgin Mountain anticline (Fig. 1) by the Eocene (Lucchitta, 1966; Young, 1966, 1979). AFT data thus provide information on the pre-extensional structural geometry and paleogeography of the region, as well as the spatial and temporal distribution of synextensional basement exhumation.

The ca. 22–20 Ma ages obtained from granite clasts in the Miocene sedimentary sequence suggest erosion of a basement source that was proximal to the basement-cover contact, since these ages are consistent with subunconformity in situ basement AFT ages. Further temporal constraints on basement exhumation are provided by facies relations within Miocene sedimentary rocks bounding the anticline.

Syntectonic Miocene Sedimentary Rocks

Oligocene-Miocene sedimentary sequences exposed in the Virgin Mountains region (Fig. 1) consist of the Rainbow Gardens (26–18 Ma) and Thumb (ca. 16–14 Ma) Members of the Horse Spring Formation and the overlying red sandstone unit (ca. 11.9–10.6 Ma) (Bohannon, 1984; Beard, 1996). The Rainbow Gardens Member consists of a lower sequence of channelized conglomeratic rocks and an upper sequence of tuffaceous fluvial and lacustrine rocks that are collectively interpreted as pre-extensional sag basin deposits (Beard, 1996). Conglomeratic sequences locally contain coarse Paleozoic and Mesozoic clasts, suggesting the presence of "moderate to abrupt relief" within the region prior to middle Miocene extension (Beard, 1996). The Thumb Member consists of a lower sequence of lacustrine and distal alluvial facies rocks and an upper sequence of coarse alluvial-fan facies rocks. Thumb Member deposits are interpreted to indicate synextensional deposition into kinematically linked strike-slip and normal fault–controlled subbasins (Beard, 1996). The red sandstone unit consists of conglomerate, fine-grained clastic strata, and fallout tuffs deposited in several small subbasins (Bohannon, 1984). The onset of extension based on ages and facies relations of Miocene stratigraphy is interpreted to be ca. 16 Ma (Beard, 1996), consistent with our evidence based on AFT dating (ca. 17 Ma).

We examined facies relations in a section of steeply dipping sedimentary rocks unconformably overlying Paleozoic and Mesozoic rocks along the north flank of Bunkerville Ridge (Figs. 2 and 8). The base of the sequence consists of scattered, poorly exposed outcrops of fine-grained limestone and siltstone. These units are overlain by a sequence of coarse-grained sandstone and conglomerate (Fig. 8). The basal parts of the conglomeratic sequence contain clasts of Paleozoic and Mesozoic sedimentary rocks, while upper parts contain large (>30 cm) subrounded Proterozoic basement clasts (Fig. 8). Stratal dips are generally >60°N, with some sections of overturned south-dipping strata.

AFT dating of basement clasts contained within this sequence (Table 1) indicates that the hosting sedimentary rocks must be younger than ca. 20 Ma. The sedimentary succession and facies relations in this sequence are similar to those described from dated Thumb Member sequences exposed on the opposite side of the Virgin Mountain anticline (Beard, 1996), and we therefore suspect that this sequence belongs to the Thumb Member. However, it is also possible that this unit belongs to the red sandstone unit (B. Bohannon, 2002, personal commun.). We therefore infer an age of <16 to >10 Ma (middle Miocene) for this sequence. The sudden appearance of coarse basement clasts within the conglomeratic unit is interpreted to indicate exposure of basement rocks on the surface in a proximal source area and erosion and deposition of basement material into alluvial fans. This suggests that basement rocks were progressively "unroofed" as recorded by this sedimentary sequence and aerially exposed within the Virgin Mountain anticline by ca. 16–10 Ma. AFT ages from basement clasts suggest that the basement from which they were derived resided at depths of ≥5 km prior to ca. 20 Ma. Using the lower age limit for this sequence (ca. 10 Ma), we derive a minimum basement exhumation rate of 500 m m.y.$^{-1}$ from ca. 20 to 10 Ma, consistent with a mixture of the pre- and post–17 Ma exhumation rates from in situ bedrock AFT samples. The recognition that strata are strongly deformed and locally overturned at this locality indicates that a component of deformation along this flank of the Virgin Mountain anticline postdates ca. 16–10 Ma.

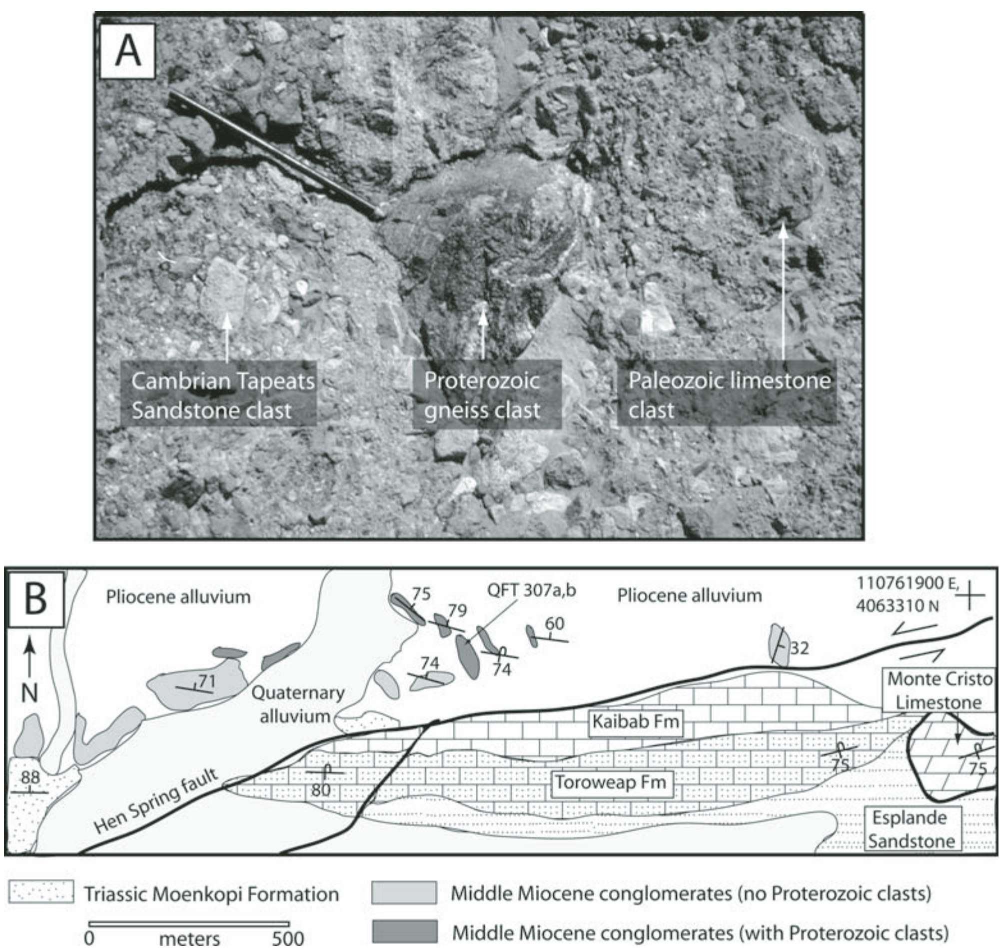

Figure 8. (A) Large Proterozoic clast in deformed Miocene conglomerates to the north of Bunkerville Ridge. Clasts of Proterozoic metasedimentary gneiss and schist, amphibolite, granite, and pegmatite are large and subangular, suggesting local derivation from the exposed Virgin Mountain anticline basement. (B) Map of red sandstone exposures and stratigraphic relationships. At the base of the conglomeratic section, no Proterozoic rocks are present; however "up-section," the frequency of Lower Cambrian and Proterozoic clasts within the conglomerate increases, to a maximum of 5%–15%. This pattern of deposition is suggestive of an unroofing sequence. Structural overturning of these rocks probably relates to left-lateral strike-slip faulting along the Hen Spring fault.

DISCUSSION

Timing of Basement Exhumation

K-feldspar $^{40}Ar/^{39}Ar$ and AFT thermochronology allow quantitative temporal constraints to be placed on the low-temperature exhumational history of the Virgin Mountain anticline. Basement rocks situated proximally beneath the Great Unconformity cooled from temperatures of ~250–300 °C to below 150 °C in the Mesoproterozoic, were exposed by the Cambrian, were buried to depths of 5–8 km prior to ca. 30 Ma (temperatures ~ 110–150 °C), were slowly exhumed through depths of <5 km from 30 to 17 Ma (temperatures < 110 °C), and were rapidly exhumed to the surface by 16–10 Ma, as indicated by the presence of these rocks in middle Miocene strata. Basement rocks at deeper structural levels preserve slightly different aspects of this tectonothermal history; some $^{40}Ar/^{39}Ar$ spectra permit the possibility that basement rocks were locally reheated to temperatures ≥150 °C after the Cambrian, and AFT data indicate that these rocks remained at temperatures ≥110 °C until rapid exhumation began at ca. 17–14 Ma. Given that the overlying Paleozoic and Mesozoic sequence was only ~4–5 km thick (Bohannon and Lucchitta, 1991; Bohannon, 1991; Bohannon et al., 1993), the possible reheating of samples to temperatures of ≥150 °C requires either (1) an elevated geotherm of >30–35 °C, or (2) Late Cretaceous tectonic thickening (i.e., thrusting) of the Paleozoic-Mesozoic sequence. Either scenario is permissible, given the presence of Laramide plutons that may have increased geothermal gradients in other parts of the transition zone (e.g., Foster et al., 1993) and the documentation of thrust sheets in the Virgin Mountain anticline region (Moore, 1972; Beard, 1993). Pre-extensional reconstructions place the Muddy Mountains thrust on top of Black Ridge at ca. 14 Ma (Duebendorfer et al., 1998), and restoration of only ~50 km of extensional translation places the Weiser syncline (Fig. 1) and related thrust ramps on top of the central part of the Virgin Mountain anticline, providing a mechanism for increased pre-extensional stratigraphic thicknesses in the region. However, the dominance of Proterozoic ages in K-feldspar spectra indicates that any thermal resetting was minimal and that basement rocks have remained in the brittle upper crust since the Proterozoic.

Regional AFT data indicate slow exhumation of Proterozoic basement in the transition zone and Colorado Plateau beginning in the Late Cretaceous and continuing to the early Miocene (≥19 Ma). Basement rocks in the Virgin Mountain anticline cooled later than basement rocks in adjacent terranes to the south and west because they were buried beneath a thicker pre-extensional sedimentary cover. Basement rocks were rapidly exhumed in the middle Miocene (17–14 Ma) at rates constrained by AFT thermal modeling of in situ samples (~630–1250 m m.y.$^{-1}$) and AFT ages of basement clasts in syn-extensional strata (≥500 m m.y.$^{-1}$). Continued ENE-WSW extension led to tilting and deformation of Miocene strata (Beard, 1996), basin subsidence (Bohannon et al., 1993), and basement uplift and erosion, as indicated by the deposition of >2 km of Neogene sediment in the Virgin River depression west of the Virgin Mountain anticline (Fig. 1; Bohannon et al., 1993).

Mechanisms of Basement Uplift and Exhumation

Structural and thermochronologic data from the Virgin Mountain anticline indicate that the primary phase of anticline uplift and exhumation occurred during the middle Miocene (Wernicke and Axen, 1988), when coeval approximately ENE-WSW extension and extension-normal N-S shortening produced a complex array of contractional, extensional, and strike-slip structures throughout the region (e.g., Wernicke et al., 1985; Wernicke and Axen, 1988; Anderson and Barnhard, 1993). The $^{40}Ar/^{39}Ar$ K-feldspar data indicate that basement rocks presently exposed throughout the Virgin Mountain anticline were exhumed from the brittle upper crust (paleodepths <7–8 km), and the absence of westward-younging trends in $^{40}Ar/^{39}Ar$ and AFT ages, together with the drape of Paleozoic strata over the northern nose of the anticline, suggests that the Virgin Mountain anticline ascended along steep bounding faults during Miocene tectonism and is not a "tilted crustal section" like the Gold Butte block.

Features such as the Western reverse fault and adjacent overturned stratigraphy along the flanks of the anticline are remarkably similar to structures of known Laramide age in the Colorado Plateau, both in terms of gross geometry and inferred shortening direction. However, the presence of overturned Miocene stratigraphy at Bunkerville Ridge suggests that these features could also have formed during Miocene tectonism. The clear signal of Miocene exhumation derived from AFT thermochronology indicates that any Laramide uplift of the Virgin Mountain anticline was minor compared to Miocene uplift. On the basis of our interpretation of the Western reverse fault and additional regional observations described previously herein, we speculate that the Virgin Mountain anticline was a low-relief (possibly <100–200 m) uplifted basement block bounded by Laramide reverse faults and overlain by Sevier thrust sheets in the Late Cretaceous to early Tertiary. The thick overlying stratigraphy and absence of major structural relief at the basement-cover interface limited bedrock exhumation at this time and kept the basement-cover interface above AFT closure temperatures (>110 °C). However, the development of basement-penetrating Laramide faults and inherited basement lithologic and structural anisotropies likely played a role in influencing the subsequent geometry of Miocene faults and, consequently, the uplift geometry of the anticline.

The gross morphology of the Virgin Mountain anticline as an uplifted, upright basement block in the footwall of a major normal fault system, together with the rapid mid-Miocene AFT cooling ages, is consistent with Wernicke and Axen's (1988) model, which shows that the anticline formed in response to the isostatic buoyancy forces associated with tectonic denudation. AFT thermochronologic data corroborate rapid removal of ≥4–5 km of bedrock from the high-standing Virgin Mountain anticline basement culminations since the middle Miocene, suggestive of coeval exhumation and uplift. Our estimated middle Miocene exhumation rates of ≥0.5–1 km $m.y.^{-1}$ together with regional structural-stratigraphic relationships suggest that basement exhumation was rapid and driven principally by tectonic denudation. Thus, the uplift of the basement-cover interface from elevations of ~0.4 km above sea level in the western Grand Canyon to elevations of >2.4 km in core of the Virgin Mountain anticline was likely driven by isostatic rebound in the footwall of the Piedmont fault–Virgin–Beaver Dam breakaway zone (Wernicke and Axen, 1988). The present geometry of the anticline and adjacent regions, however, suggests a significantly more complex tectonic history than simple isostatic footwall uplift.

The undulating dome-saddle-dome geometry observed along the axis of the Virgin Mountain anticline is commonly observed in extensional metamorphic core complexes (e.g., Spencer, 1984; Davis and Lister, 1988; Fletcher et al., 1995) and adjacent to rift zones (e.g., May et al., 1994; Lewis and Baldridge, 1994) and is commonly attributed to buckling in response to increased horizontal compression perpendicular to the extension direction (Fletcher et al., 1995). The abundance of structures indicating N-S contraction throughout the study region (Wernicke et al., 1985; Anderson and Barnhard, 1993) confirms that extension-normal contraction is likely to have contributed to the formation of the undulating geometry characterizing the Virgin Mountain anticline. Tectonic and erosional denudation of the Virgin Mountain anticline may have reduced the vertical normal stress to sufficient levels to facilitate extension-perpendicular buckling (e.g., Fletcher et al., 1995). We therefore suggest that, in addition to isostatically driven uplift, an unconstrained component of anticline uplift (and perhaps downwarping in saddle areas) relates to extension-normal shortening during crustal extension (Wernicke et al., 1985; Anderson and Barnhard, 1993).

The structural topography lows to the west of the Virgin Mountain anticline and in the region between the anticline and the Grand Wash fault reflect crustal extension, large dip-slip normal fault displacements, and resultant basin formation (Bohannon et al., 1993). Langenheim et al. (2001) suggested that the Virgin River depression formed due to the lateral westward flow of mid- and lower crust from beneath the basin. This hypothesis was based on the observation that upper-crustal thickness appears to vary little between extended blocks in the basin and bounding ranges, despite the major differences in structural elevation.

The extent to which strike-slip faulting played a role in contributing to the present geometry of the anticline is uncertain. Some estimates of strike slip are based on offset basement lithologies or basement "piercing points" (e.g., Williams et al., 1997; Bohannon, 1979); however, most basement-penetrating faults reactivated Proterozoic dextral shear zones that may have had multiple displacement histories prior to any Miocene slip, and thus reliance upon measurements of offset basement lithologies is unreliable (Quigley, 2002). We suspect that the primary role of strike-slip deformation in the study region was to accommodate N-S contraction (Anderson and Barnhard, 1993) and/or lateral variations in extension magnitude via linkage with normal faults (i.e., transfer faults; Duebendorfer and Black, 1992; Duebendorfer et al., 1998; Beard, 1996) and that strike-slip faulting played a minimal role relative to isostasy and N-S shortening in driving basement uplift. However, the presence of exhumed basement clasts in sedimentary sequences deformed by strike-slip faults (Fig. 8; Beard, 1996) suggests that major strike-slip structures such as the Hen Spring fault may have modified and segmented the anticline following its formation, resulting in the complex geometry observed at present.

The presence of basement-cover detachment zones such as the Mount Bangs detachment suggests that tectonism, and possible decoupling of basement from cover associated with low-angle faults, was an important process during the evolution of the Virgin Mountain anticline. Kinematic analysis of the Mount Bangs detachment suggests that an episode of top-to-the-east normal faulting may have predated or been synchronous with the early stages of anticline formation. The intensity of deformation associated with these zones, as indicated by the thickness of fault gouge and removal of several hundreds of meters of bedrock material within the Mount Bangs detachment, as well as the presence of similar structures in the Gold Butte block (Karlstrom et al., this volume), suggests that these features are likely to have incurred large-magnitude displacements over regional extents, and they should be considered in future tectonic models of the region.

CONCLUSIONS

The Virgin Mountain anticline is an uplifted, upright basement block situated in the footwall of a major normal fault system within the Colorado Plateau–Basin and Range transition zone. The $^{40}Ar/^{39}Ar$ K-feldspar and apatite fission-track thermochronology presented here indicates that basement rocks within the core of the anticline were rapidly exhumed from depths of ~5–8 km beginning at ca. 17 Ma, and this age is interpreted to mark the onset of rapid ENE-WSW extension in the region. The apparently complex geometry of the anticline resulted from the superposition of first-order processes, including isostatic footwall uplift and extension-perpendicular shortening, on a previously tectonized and strongly anisotropic crust. A small basement-cored uplift may have formed during the Laramide orogeny, but the bulk of uplift, exhumation, and deformation of the Virgin Mountain anticline occurred during middle Miocene tectonism.

ACKNOWLEDGMENTS

We thank all those who have commented on various forms of this manuscript since its initial inception as Quigley's Master's thesis in 2002. These include Brian Wernicke, Michael Wells, Paul Umhoefer, David Foster, Keith Howard, Joan Fryxell, Yildirim Dilek, Chuck Naeser, Ernie Anderson, Sue Beard, and Bob Bohannon. This paper also profited from discussions with many of those that attended Quigley's toothless Geological Society of America field trip to the Virgin Mountains in 2002.

REFERENCES CITED

Anderson, R.E., 1973, Large-Magnitude Late Tertiary Strike-Slip Faulting North of Lake Mead, Nevada: U.S. Geological Survey Professional Paper 794, 18 p.

Anderson, R.E., and Barnhard, T.P., 1993, Aspects of three-dimensional strain at the margin of the extensional orogen, Virgin River depression area, Nevada, Utah, and Arizona: Geological Society of America Bulletin, v. 105, p. 1019–1052, doi: 10.1130/0016-7606(1993)105<1019:AOTDSA>2.3.CO;2.

Anderson, R.E., Barnhard, T.P., Snee, L.W., 1994, Roles of plutonism, mid-crustal flow, tectonic rafting, and horizontal collapse in shaping the Miocene strain field of the Lake Mead area, Nevada and Arizona: Tectonics, v. 13, no. 6, p. 1381–1410.

Axen, G.J., 1991, Tertiary Extension, Magmatism, and Thrust Reactivation in the Southern Great Basin, and a Mechanical Model for Detachment Faulting [Ph.D. thesis]: Cambridge, Massachusetts, Harvard University, 235 p.

Axen, G.J., Wernicke, B.P., Taylor, W.J., and Skelly, M.F., 1990, Mesozoic and Cenozoic tectonics of the Sevier thrust belt in the Virgin River Valley area, southern Nevada, *in* Wernicke, B.P., ed., Basin and Range Extension near the Latitude of Las Vegas, Nevada: Geological Society of America Memoir 176, p. 123–154.

Beal, L.H., 1965, Geology and Mineral Deposits of the Bunkerville Mining District, Clark County, Nevada: Bulletin of the Nevada Bureau of Mines 63, 96 p.

Beard, L.S., 1993, Geologic Map of the Whitney Pocket 7.5-Minute Quadrangle, Clark County, Nevada: U.S. Geological Survey Open-File Report 93-716, 15 p., scale 1:24,000.

Beard, L.S., 1996, Paleogeography of the Horse Spring Formation in relation to the Lake Mead fault system, *in* Beratan, K.K., ed., Reconstructing the History of Basin and Range Extension Using Sedimentology and Stratigraphy: Geological Society of America Special Paper 303, p. 27–60.

Bennett, V.C., and DePaolo, D.J., 1987, Proterozoic crustal history of the western United States as determined by neodymium isotopic mapping: Geological Society of America Bulletin, v. 99, p. 674–685, doi: 10.1130/0016-7606(1987)99<674:PCHOTW>2.0.CO;2.

Bohannon, R.G., 1979, Strike-slip faults of the Lake Mead region of southern Nevada, *in* Armentrout, J.M., Cole, M.R., and Ter Best, H., Jr., eds., Cenozoic Paleogeography of the Western United States: Pacific Coast Paleogeography Symposium: Anaheim, California, Society of Economic Paleontologists and Mineralogists, Pacific Section, p. 129–139.

Bohannon, R.G., 1984, Nonmarine Sedimentary Rocks of Tertiary Age in the Lake Mead Region, Southeastern Nevada and Northwestern Arizona: U.S. Geological Survey Professional Paper 1259, 72 p.

Bohannon, R.G., 1991, Geologic Map of the Jacobs Well and Southern Part of the Elbow Canyon Quadrangles, Mohave County, Arizona: U.S. Geological Survey Miscellaneous Investigations Series Map I-2167, scale 1:24,000.

Bohannon, R.G., and Lucchitta, I., 1991, Geologic Map of the Mount Bangs Quadrangle, Mohave County, Arizona: U.S. Geological Survey Miscellaneous Investigations Series Map I-2166, scale 1:24,000.

Bohannon, R.G., Grow, J.A., Miller, J.J., and Blank, R.H., Jr., 1993, Seismic stratigraphy and tectonic development of Virgin River depression and associated basin, southeastern Nevada and northwestern Arizona: Geological Society of America Bulletin, v. 105, p. 501–520, doi: 10.1130/0016-7606(1993)105<0501:SSATDO>2.3.CO;2.

Brady, R., 2005, Ongoing studies of tilting and uplift in the South Virgin Mountains, Nevada: Geological Society of America Abstracts with Programs, v. 37, no. 7, p. 128.

Brady, R., Wernicke, B.P., and Fryxell, J.E., 2000, Kinematic evolution of a large-offset continental normal fault system, South Virgin Mountains, Nevada: Geological Society of America Bulletin, v. 112, p. 1375–1397.

Bryant, B., Naeser, C.W., and Fryxell, J.E., 1991, Implications of low-temperature cooling history on a transect across the Colorado Plateau–Basin and Range boundary, west central Arizona: Journal of Geophysical Research, v. 96, p. 12,375–12,388.

Campagna, D.J., and Aydin, A., 1994, Basin genesis associated with strike-slip faulting in the Basin and Range, southeastern Nevada: Tectonics, v. 13, p. 327–341, doi: 10.1029/93TC02723.

Carter, T.J., Kohn, B.P., Foster, D.A., and Gleadow, A.J.W., 2004, How the Harcuvar Mountains metamorphic core complex became cool: Evidence from apatite (U-Th)/He thermochronometry: Geology, v. 32, p. 985–988, doi: 10.1130/G20936.1.

Carter, T.J., Kohn, B.P., Foster, D.A., Gleadow, A.J.W., and Woodhead, J.D., 2006, Late-stage evolution of the Chemehuevi and Sacramento detachment faults from apatite (U-Th)/He thermochronometry—Evidence for accelerated slip at ca. 15 Ma: Geological Society of America Bulletin, v. 118, p. 689–709, doi: 10.1130/B25736.1.

Davis, G.A., and Lister, G.S., 1988, Detachment faulting in continental extension: Perspectives from the southwestern U.S. Cordillera, *in* Clark, S.P., Jr., Burchfiel, B.C., and Suppe, J., eds., Processes in Continental Lithospheric Deformation: Geological Society of America Special Paper 218, p. 133–159.

Duebendorfer, E., and Black, R., 1992, Kinematic role of transverse structures in continental extension: An example from the Las Vegas Valley shear zone, Nevada: Geology, v. 20, p. 1107–1110, doi: 10.1130/0091-7613(1992)020<1107:KROTSI>2.3.CO;2.

Duebendorfer, E., and Wallin, E.T., 1991, Basin development and syntectonic sedimentation associated with kinematically coupled strike-slip and detachment faulting, southern Nevada: Geology, v. 19, p. 87–90, doi: 10.1130/0091-7613(1991)019<0087:BDASSA>2.3.CO;2.

Duebendorfer, E.M., Beard, L.S., and Smith, E.I., 1998, Restoration of Tertiary deformation in the Lake Mead region, southern Nevada: The role of strike-slip transfer faults, *in* Faulds, J.E., and Stewart J.H., eds., Accommodation Zones and Transfer Zones: The Regional Segmentation of the Basin and Range Province: Geological Society of America Paper 323, p. 127–148.

Fitzgerald, P.G., Fryxell, J.E., and Wernicke, B.P., 1991, Miocene crustal extension and uplift in southeastern Nevada: Constraints from fission-track analysis: Geology, v. 19, p. 1013–1016, doi: 10.1130/0091-7613(1991)019<1013:MCEAUI>2.3.CO;2.

Fletcher, J.M., Bartley, J.M., Martin, M.W., Glazner, A.F., and Walker, J.D., 1995, Large-magnitude continental extension: An example from the central Mojave metamorphic core complex: Geological Society of America Bulletin, v. 107, p. 1468–1483, doi: 10.1130/0016-7606(1995)107<1468:LMCEAE>2.3.CO;2.

Foster, D.A., and Gleadow, A.J., 1992, The morphotectonic evolution of rift-margin mountains in central Kenya—Constraints from apatite fission-track thermochronology: Earth and Planetary Science Letters, v. 113, p. 157–171, doi: 10.1016/0012-821X(92)90217-J.

Foster, D.A., and John, B.E., 1999, Quantifying tectonic exhumation in an extensional orogen with thermochronology: Examples from the southern Basin and Range Province, *in* Ring, U., Brandon, M., Lister, G.S., and Willett, S.D., eds., Exhumation Processes: Normal Faulting, Ductile Flow, and Erosion: Geological Society of London Special Publication 154, p. 356–378.

Foster, D.A., Harrison, T.M., Miller, C.F., and Howard, K.A., 1990, ^{40}Ar/^{39}Ar thermochronology of the eastern Mojave Desert, California, and adjacent western Arizona with implications for the evolution of metamorphic core complexes: Journal of Geophysical Research, v. 95, p. 20,005–20,024, doi: 10.1029/JB095iB12p20005.

Foster, D.A., Gleadow, A.J., Reynolds, S.J., and Fitzgerald, P.G., 1993, Denudation of metamorphic core complexes and the reconstruction of the transition zone, west central Arizona: constraints from apatite fission-track thermochronology: Journal of Geophysical Research, v. 98, p. 2167–2185, doi: 10.1029/92JB02407.

Fryxell, J., Salton, G., Selverstone, J., and Wernicke, B., 1992, Gold Butte crustal section, South Virgin Mountains, Nevada: Tectonics, v. 11, p. 1099–1120, doi: 10.1029/92TC00457.

Galbraith, R.F., 1981, On statistical models of fission-track counts: Mathematical Geology, v. 13, p. 471–478, doi: 10.1007/BF01034498.

Green, P.F., Duddy, I.R., Laslett, G.M., Hegarty, K.A., Gleadow, A.J., and Lovering, J.F., 1989, Thermal annealing of fission-tracks in apatite: 4. Quantitative modeling techniques and extension to geological timescales: Chemical Geology, Isotope Geoscience Section, v. 79, p. 155–182, doi: 10.1016/0168-9622(89)90018-3.

Hintze, L.F., 1986, Stratigraphy and structure of the Beaver Dam Mountains, southwestern Utah, *in* Griffen, D.T., and Philips, W.R., eds., Thrusting and Extensional Structures and Mineralization in the Beaver Dam Mountains, Southwestern Utah: Utah Geological Association Publication 15, p. 69–76.

Huntoon, P.W., 1990, Phanerozoic structural geology of the Grand Canyon: Grand Canyon Geology, p. 261–309.

Huntoon, P.W., 1990, Phanerozoic structural geology of the Grand Canyon, *in* Beus, S.S., and Morales, M., eds., Grand Canyon Geology: New York, Oxford University Press, p. 261–309.

Hurford, A.J., and Green, P.F., 1983, The zeta age calibration of fission-track dating: Chemical Geology, v. 1, p. 285–317.

Ilg, B., Karlstrom, K.E., Hawkins, D.P., and Williams, M.L., 1996, Tectonic evolution of Paleoproterozoic rocks in the Grand Canyon: Insights into middle-crustal processes: Geological Society of America Bulletin, v. 108, p. 1149–1166, doi: 10.1130/0016-7606(1996)108<1149:TEOPRI>2.3.CO;2.

Kamilli, R.J., and Richard, S.M., eds., 1998, Geologic Highway Map of Arizona: Tucson, Arizona, Arizona Geological Society and Arizona Geological Survey, 1 sheet containing text and figures, scale 1:1,000,000.

Karlstrom, K.E., Quigley, M.C., Bowring, S.A., Hook, S., Kirby, E., and Heizler, M., 2001, Low angle detachment along the Great Unconformity near the Colorado Plateau–Basin and Range breakaway: Arguments against a tipped crustal section in the Gold Butte area, southern Nevada, *in* Erskine, M.C., Faulds, J.E., Bartley, J.M., and Rowley, P.D., eds., The Geologic Transition, High Plateaus to Great Basin—A Symposium and Field Guide: The Mackin Volume: Pacific Section, American Association of Petroleum Geologists Guidebook 78, p. 425.

Karlstrom, K.E., Matt Heizler, M., and Quigley, M.C., 2010, this volume, Structure and $^{40}Ar/^{39}Ar$ K-feldspar thermal history of the Gold Butte block: Reevaluation of the tilted crustal section model, *in* Umhoefer, P.J., Beard, L.S., and Lamb, M.A., eds., Miocene Tectonics of the Lake Mead Region, Central Basin and Range: Geological Society of America Special Paper 463, doi: 10.1130/2010.2463(15).

Kelley, S.A., and Chapin, C.E., 2004, Denudational histories of the Front Range and Wet Mountains, Colorado, based on apatite fission-track thermochronology, *in* Cather, S.M., McIntosh, W., and Kelley, S.A., eds., Tectonics, Geochronology and Volcanism in the Southern Rocky Mountains and Rio Grande Rift: New Mexico Bureau of Geology and Mineral Resources Bulletin 160, p. 41–77.

Kelley, S.A., Chapin, C.E., and Corrigan, J., 1992, Late Mesozoic to Cenozoic Cooling Histories of the Flanks of the Northern and Central Rio Grande Rift, Colorado and New Mexico: New Mexico Bureau of Mines and Mineral Resources Bulletin 145, 39 p.

Kelley, S.A., Chapin, C.E., and Karlstrom, K.E., 2000, Laramide cooling histories of the Grand Canyon, Arizona, and the Front Range, Colorado: Geological Society of America Abstracts with Programs, v. 32, no. 7, p. 42.

Kelley, S.A., Chapin, C.E., and Karlstrom, K.E., 2001, Laramide cooling histories of the Grand Canyon, Arizona, and the Front Range, Colorado, determined from apatite fission-track thermochronology, *in* Young, R.A., and Spamer, E.E., eds., Colorado River: Origin and Evolution: Grand Canyon, Arizona, Grand Canyon Association, p. 37–42.

Ketcham, R.A., Donelick, R.A., and Donelick, M.B., 2000, AFTSolve: A program for multi-kinetic modeling of apatite fission-track data: Geological Materials Research, v. 2, p. 1–32.

Kruse, S., McNutt, M., Phipps-Morgan, J., and Royden, L., 1991, Lithospheric extension near Lake Mead, Nevada: A model for ductile flow in the lower crust: Journal of Geophysical Research, v. 96, p. 4435–4456, doi: 10.1029/90JB02621.

Langenheim, V.E., Bohannon, R.G., Glen, J.M., Jachens, R.C., Grow, J.A., Miller, J.J., Dixon, G.L., and Katzer, T.C., 2001, Basin configuration of the Virgin River depression, Nevada, Utah, and Arizona: A geophysical view of deformation along the Colorado Plateau–Basin and Range transition, *in* Erskine, M.C., Faulds, J.E., Bartley, J.M., and Rowley, P.D., eds., The Geologic Transition, High Plateaus to Great Basin—A Symposium and Field Guide: The Mackin Volume: Pacific Section, American Association of Petroleum Geologists Guidebook 78, p. 205–226.

Laslett, G.M., Kendall, W.S., Gleadow, A.J.W., and Duddy, I.R., 1982, Bias in measurement of fission track length distributions: Nuclear Tracks, v. 6, p. 79–85.

Lewis, C.J., and Baldridge, W.S., 1994, Crustal extension in the Rio Grande rift, New Mexico: Half-grabens, accommodation zones, and shoulder uplifts in the Ladron Peak–Sierra Lucero area, *in* Keller, G.R., and Cather, S.M., eds., Basins of the Rio Grande Rift: Structure, Stratigraphy, and Tectonic Setting: Geological Society of America Special Paper 291, p. 135–156.

Lister, G.S., and Baldwin, S.L., 1996, Modelling the effect of arbitrary *P-T-t* histories on argon diffusion in minerals using the MacArgon program for the Apple Macintosh: Tectonophysics, v. 253, p. 83–109, doi: 10.1016/0040-1951(95)00059-3.

Longwell, C.R., Pampeyan, E.H., Bower, B., and Roberts, R.J., 1965, Geology and Mineral Deposits of Clark County, Nevada: Nevada Bureau of Mines Bulletin 62, 218 p.

Lovera, O.M., Richter, F.M., and Harrison, T.M., 1989, The $^{40}Ar/^{39}Ar$ thermochronometry for slowly cooled samples having a distribution of diffusion domain sizes: Journal of Geophysical Research, v. 94, p. 17,917–17,935, doi: 10.1029/JB094iB12p17917.

Lucchitta, I., 1966, Cenozoic Geology of the Upper Lake Mead Area Adjacent to the Grand Wash Cliffs, Arizona [Ph.D. thesis]: University Park, Pennsylvania State University, 218 p.

Marshak, S., Karlstrom, K.E., and Timmons, M.J., 2000, Inversion of Proterozoic extensional faults: An explanation for the patterns of Laramide and Ancestral Rockies intracratonic deformation, USA: Geology, v. 28, p. 735–738, doi: 10.1130/0091-7613(2000)28<735:IOPEFA>2.0.CO;2.

May, S.J., Kelley, S.A., and Russell, L.R., 1994, Footwall unloading and rift shoulder uplifts in the Albuquerque Basin: Their relation to syn-rift fanglomerates and apatite fission-track ages, *in* Keller, G.R., and Cather, S.M., eds., Basins of the Rio Grande Rift: Structure, Stratigraphy, and Tectonic Setting: Geological Society of America Special Paper 291, p. 125–134.

McDougall, I., and Harrison, T.M., 1999, Geochronology and Thermochronology by the $^{40}Ar/^{39}Ar$ Method: New York, Oxford University Press, 212 p.

Michel-Noel, G., 1988, Mecanismes et Evolution de l'Extension Intracontinentale des Basins and Range, et Developpement Tectonique des Basins Sedimentaires [thesis]: Paris, France, Academie de Paris, Université Pierre et Marie Curie, Memoires des Sciences de la Terre, 205 p.

Moore, R.T., 1972, Geology of the Virgin and Beaver Dam Mountains, Arizona: Arizona Bureau of Mines Bulletin 186, 65 p.

Naeser, C.W., 1979, Fission-track dating and geologic annealing of fission-tracks, *in* Jager, E., and Hunziker, J.C., eds., Lectures in Isotope Geology: New York, Springer Verlag, p. 154–169.

Naeser, C.W., Duddy, I.R., Elston, D.P., Dumitru, T.A., and Green, P.F., 1989, Chapter 17: Fission-track dating: Ages for Cambrian strata and Laramide and post–middle Eocene cooling events from the Grand Canyon, Arizona, *in* Elston, D.P., Billingsley, G.H., and Young, R.A., eds., Geology of the Grand Canyon, Northern Arizona (with Colorado River Guides): Washington, D.C., American Geophysical Union, p. 139–144.

O'Sullivan, P., Carpenter, D.G., and Carpenter, J.A., 1994, Cooling history of the Beaver Dam Mountains, Utah: Determined by apatite fission-track analysis, *in* Dobbs, S.W., and Taylor, W.J., eds., Structural and Stratigraphic Investigations and Petroleum Potential of Nevada, with Special Emphasis South of the Railroad Valley Producing Trend: Reno, Nevada, Nevada Petroleum Society, p. 53–64.

Powell, J.W., 1875, Exploration of the Colorado River of the West and Its Tributaries: Washington, D.C., U.S. Government Printing Office, 291 p.

Press, W.H., Flannery, B.P., Teukolsky, S.A., and Vetterling, W.T., 1988, Numerical Recipes: Cambridge, UK, Cambridge University Press, 965 p.

Quigley, M.C., 2002, Tectonic Development of Proterozoic Structures and Their Influence on Laramide and Miocene Deformation, North Virgin Mountains, SE Nevada and NW Arizona [M.S. thesis]: Albuquerque, University of New Mexico, 194 p.

Quigley, M.C., Karlstrom, K.E., Beard, S., and Bohannon, R.G., 2002, Influence of Proterozoic and Laramide structures on the Miocene extensional strain field, North Virgin Mountains, Nevada/Arizona, *in* Lund, W., ed., Field Guide to Geologic Excursions in Southwestern Utah and Adjacent Areas of Arizona and Nevada: U.S. Geological Survey Open-File Report 02-172, p. 85–104.

Reiners, P.W., and Farley, K.A., 1999, He diffusion and (U-Th)/He thermochronometry of titanite: Geochimica et Cosmochimica Acta, v. 63, p. 3845–3859, doi: 10.1016/S0016-7037(99)00170-2.

Reiners, P.W., Brady, R., Farley, K.A., Fryxell, J.E., Wernicke, B., and Lux, D., 2000, Helium and argon thermochronometry of the Gold Butte block, South Virgin Mountains, Nevada: Earth and Planetary Science Letters, v. 178, p. 315–326, doi: 10.1016/S0012-821X(00)00080-7.

Seager, W., 1970, Low-angle gravity slide structures in the northern Virgin Mountains, Nevada: Geological Society of America Bulletin, v. 81, p. 1517–1538, doi: 10.1130/0016-7606(1970)81[1517:LGGSIT]2.0.CO;2.

Silver, L.T., Bickford, M.E., Van Schmus, W.R., Anderson, J.L., Anderson, T.H., and Medaris, L.G., Jr, 1977, The 1.4–1.5 b.y. transcontinental anorogenic plutonic perforation of North America: Geological Society of America Abstracts with Programs, v. 9, n. 7, p. 1176–1177.

Spencer, J.E., 1984, Role of tectonic denudation in warping an uplift of low-angle normal faults: Geology, v. 12, p. 95–98, doi: 10.1130/0091-7613(1984)12<95:ROTDIW>2.0.CO;2.

Stockli, D.F., 1999. Regional Timing and Spatial Distribution of Miocene Extension in the Northern Basin and Range Province: Stanford, California, Stanford University, 239 p.

Timmons, M.J., Karlstrom, K.E., Dehler, C.M., Geissman, J.W., and Heizler, M.T., 2001, Proterozoic multistage (~1.1 and ~0.8 Ga) extension in the Grand Canyon Supergroup and establishment of northwest and north-south tectonic grains in the southwestern United States: Geological Society of America Bulletin, v. 113, p. 163–180, doi: 10.1130/0016-7606(2001)113<0163:PMCAGE>2.0.CO;2.

Timmons, J.M., Karlstrom, K.E., Heizler, M.T., Bowring, S.A., Gehrels, G.E., and Crossey, L.J., 2005, Tectonic inferences from the ca. 1255–1100 Ma Unkar Group and Nankoweap Formation, Grand Canyon: Intracratonic deformation and basin formation during protracted Grenville orogenesis: Geological Society of America Bulletin, v. 117, p. 1573–1595, doi: 10.1130/B25538.1.

Wasserburg, G.A., and Lamphere, M.A., 1965, Age determinations in the Precambrian of Arizona and Nevada: Geological Society of America Bulletin, v. 76, p. 735–758, doi: 10.1130/0016-7606(1965)76[735:ADITPO]2.0.CO;2.

Wernicke, B.P., and Axen, G.J., 1988, On the role of isostasy in the evolution of normal fault systems: Geology, v. 16, p. 848–851, doi: 10.1130/0091-7613(1988)016<0848:OTROII>2.3.CO;2.

Wernicke, B., Guth, P.L., and Axen, G.J., 1984, Tertiary extension in the Sevier orogenic belt, southern Nevada, *in* Lintz, J.P., ed., Western Geological Excursions: Reno, Nevada, MacKay School of Mines, v. 4, p. 473–510.

Wernicke, B.P., Walker, J.D., and Beaufait, M.S., 1985, Structural discordance between Neogene detachments and frontal Sevier thrusts, central Mormon Mountains, southern Nevada: Tectonics, v. 4, p. 213–246, doi: 10.1029/TC004i002p00213.

Wernicke, B.P., Axen, G.J., and Snow, J.K., 1988, Basin and Range extensional tectonics at the latitude of Las Vegas, Nevada: Geological Society of America Bulletin, v. 100, p. 1738–1757, doi: 10.1130/0016-7606(1988)100<1738:BARETA>2.3.CO;2.

Williams, V.S., Bohannon, R.G., and Hoover, D.L., 1997, Geologic Map of the Riverside Quadrangle, Clark County, Nevada: U.S. Geological Survey Geologic Map GQ-1770, scale 1:24,000.

Willett, S.D., 1992, Modelling thermal annealing of fission-tracks in apatite, *in* Zentilli, M., and Reynolds, P.H., eds., Short Course Handbook on Low Temperature Thermochronology: Quebec, Mineralogical Association of Canada, p. 43–72.

Willett, S.D., 1997, Inverse modeling of annealing of fission-tracks in apatite: 1. A controlled random search method: American Journal of Science, v. 297, p. 939–969.

Young, R.A., 1966, Cenozoic Geology along the Edge of the Colorado Plateau in Northwestern Arizona, [Ph.D. thesis]: St. Louis, Missouri, Washington University, 167 p.

Young, R.A., 1979, Laramide deformation, erosion and plutonism along the southwestern margin of the Colorado Plateau: Tectonophysics, v. 61, p. 25–47, doi: 10.1016/0040-1951(79)90290-7.

Young, R.A., 2001, Geomorphic, structural, and stratigraphic evidence for Laramide uplift of the southwestern Colorado Plateau margin of NW Arizona, *in* Erskine, M.C., Faulds, J.E., Bartley, J.M., and Rowley, P.D., eds., The Geologic Transition, High Plateaus to Great Basin—A Symposium and Field Guide: The Mackin Volume: Pacific Section, American Association of Petroleum Geologists Guidebook 78, p. 227–237.

Manuscript Accepted by the Society 17 August 2009